

DTIC FILE COPY

(2)

# NAVAL POSTGRADUATE SCHOOL

## Monterey, California

AD-A202 698



DTIC  
SELECTED  
18 JAN 1989  
S E D  
Cp E

## THESIS

ANALYTICAL AND EXPERIMENTAL  
INVESTIGATION OF CONSTRAINED  
VISCOELASTIC LAYER DAMPING FOR  
A PLATE AND SHELL MODEL

by  
James R. Nault  
September 1988

Thesis Advisor:

Y.S. Shin

Approved for public release; distribution is unlimited

89 1 17 215

UNCLASSIFIED

SECURITY CLASSIFICATION OF THIS PAGE

HD A-1

REPORT DOCUMENTATION PAGE			
1a REPORT SECURITY CLASSIFICATION  UNCLASSIFIED		1b RESTRICTIVE MARKINGS	
2a SECURITY CLASSIFICATION AUTHORITY		3 DISTRIBUTION/AVAILABILITY OF REPORT Approved for public release; distribution is unlimited.	
2b DECLASSIFICATION/DOWNGRADING SCHEDULE			
4 PERFORMING ORGANIZATION REPORT NUMBER(S)		5 MONITORING ORGANIZATION REPORT NUMBER(S)	
6a NAME OF PERFORMING ORGANIZATION  Naval Postgraduate School	6b OFFICE SYMBOL  (if applicable) 69	7a NAME OF MONITORING ORGANIZATION  Naval Postgraduate School	
6c ADDRESS (City, State, and ZIP Code)  Monterey, California 93943-5000		7b ADDRESS (City, State, and ZIP Code)  Monterey, California 93943-5000	
8a NAME OF FUNDING / SPONSORING ORGANIZATION	8b OFFICE SYMBOL  (if applicable)	9 PROCUREMENT INSTRUMENT IDENTIFICATION NUMBER	
8c ADDRESS (City, State, and ZIP Code)		10 SOURCE OF FUNDING NUMBERS	
		PROGRAM ELEMENT NO	PROJECT NO
		TASK NO	WORK UNIT ACCESSION NO
11 TITLE (Include Security Classification) Analytical and Experimental Investigation of Constrained Viscoelastic Layer Damping for a Plate and Shell Model			
12 PERSONAL AUTHOR(S) Nault, James R.			
13 TYPE OF REPORT Masters Thesis	14 DATE OF REPORT (Year Month Day) 1988 September	15 PAGE COUNT 96	
16 SUPPLEMENTARY NOTATION The views expressed in this thesis are those of the author and do not reflect the official policy or position of the Department of Defense or the U.S. Government.			
17 COSATI CODES		18 SUBJECT TERMS (Continue on reverse if necessary and identify by block number) Constrained Layer Damping, Plates, and Shells Finite Element Modeling • (nigm) ←	
19 ABSTRACT (Continue on reverse if necessary and identify by block number)  The use of constrained viscoelastic layer damping treatments has recently been found to be effective in reducing unwanted resonant vibrations in structures. The proper design of such damping treatments has been difficult, however, since closed form equations to describe system behavior can only be used for simple beams and plates. In addition, finite element analysis has been difficult since the material properties of viscoelastic materials show a marked dependence on frequency and temperature, resulting in the need to run an excessive number of finite element analyses for each design. Two recently developed design tools are used in this paper to design a proper constrained viscoelastic layer damping treatment for a test structure consisting of two concentric cylinders connected by four vanes. The first design tool is subsystem analysis, where a portion of the test structure is approximated by appropriate closed			
20 DISTRIBUTION AVAILABILITY OF ABSTRACT <input checked="" type="checkbox"/> UNCLASSIFIED/UNLIMITED <input type="checkbox"/> SAME AS RPT <input type="checkbox"/> DTIC USERS		21 ABSTRACT SECURITY CLASSIFICATION UNCLASSIFIED	
22a NAME OF RESPONSIBLE INDIVIDUAL Professor Young S. Shin		22b TELEPHONE (Include Area Code) (408)-646-2568	22c OFFICE SYMBOL 69SG

Unclassified

SECURITY CLASSIFICATION OF THIS PAGE (When Data Entered)

Block 19 cont.

form equations to determine system behavior with different applied damping treatments. The second design tool is a finite element technique called the Modal Strain Energy method.

After application of the constrained viscoelastic layer damping treatment to the outer shell of the test structure, vibration response amplitudes were found to drop significantly for all frequencies except in the lowest fifth of the frequency range. This was due to the low shear modulus of the viscoelastic material at these low frequencies, which made the viscoelastic material unable to provide good shear resistance. Structural damping also increased. Further application of damping treatments to the vanes of the structure produced only slightly more damping and response amplitude reduction.

The Modal Strain Energy method did not show good agreement with the experimental results. In general, the Modal Strain Energy method was a conservative design tool in that it predicted higher responses and less damping for the test structure than was obtained experimentally. Errors in the Modal Strain Energy analysis were due to coarseness of the finite element model and inaccuracy in the modeling of the bolted joints of the structure.

S N 0102-LF-014-6601

Unclassified

SECURITY CLASSIFICATION OF THIS PAGE (When Data Entered)

Approved for Public release: distribution is unlimited.

**ANALYTICAL AND EXPERIMENTAL INVESTIGATION OF  
CONSTRAINED VISCOELASTIC LAYER DAMPING FOR A  
PLATE AND SHELL MODEL**

by

James Robert Nault  
Lieutenant, United States Navy  
B.S.M.E., United States Naval Academy, 1981

Submitted in partial fulfillment of the  
requirements for the degree of

**MASTER OF SCIENCE IN MECHANICAL ENGINEERING**

from the

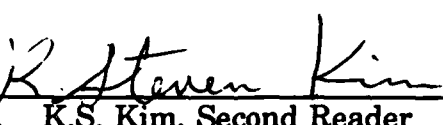
**NAVAL POSTGRADUATE SCHOOL**  
September 1988

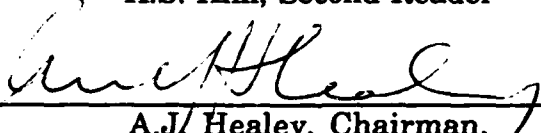
Author:

  
James Robert Nault

Approved by:

  
Y.B. Shin, Thesis Advisor

  
K. Steven Kim  
K.S. Kim, Second Reader

  
A.J. Healey, Chairman,  
Department of Mechanical Engineering

  
Gordon E. Schacher,  
Dean of Science and Engineering

## **ABSTRACT**

The use of constrained viscoelastic layer damping treatments has recently been found to be effective in reducing unwanted resonant vibrations in structures. The proper design of such damping treatments has been difficult, however, since closed form equations to describe system behavior can only be used for simple beams and plates. In addition, finite element analysis has been difficult since the material properties of viscoelastic materials show a marked dependence on frequency and temperature, resulting in the need to run an excessive number of finite element analyses for each design. Two recently developed design tools are used in this paper to design a proper constrained viscoelastic layer damping treatment for a test structure consisting of two concentric cylinders connected by four vanes. The first design tool is subsystem analysis, where a portion of the test structure is approximated by appropriate closed form equations to determine system behavior with different applied damping treatments. The second design tool is a finite element technique called the Modal Strain Energy method.

After application of the constrained viscoelastic layer damping treatment to the outer shell of the test structure, vibration response amplitudes were found to drop significantly for all frequencies except in the lowest fifth of the frequency range. This was due to the low shear modulus of the viscoelastic material at these low frequencies, which made the viscoelastic material unable to provide good shear resistance. Structural damping also increased. Further application of damping treatments to the vanes of the structure produced only slightly more damping and response amplitude reduction.

The Modal Strain Energy method did not show good agreement with the experimental results. In general, the Modal Strain Energy method was a conservative design tool in that it predicted higher responses and less damping for the test structure than was obtained experimentally. Errors in

the Modal Strain Energy analysis were due to coarseness of the finite element model and inaccuracy in the modeling of the bolted joints of the structure.

Accession For	
NTIS GRA&I	<input checked="" type="checkbox"/>
DTIC TAB	<input type="checkbox"/>
Unannounced	<input type="checkbox"/>
Justification	
By _____	
Distribution/ _____	
Availability Codes	
Dist	Avail and/or Special
A-1	



## TABLE OF CONTENTS

I.	INTRODUCTION	1
A.	BACKGROUND	1
B.	PURPOSE	2
II.	THEORY	3
A.	EQUATIONS OF MOTION AND VIBRATION MODES	3
B.	VISCOELASTIC DAMPING	6
C.	MODAL STRAIN ENERGY METHOD	9
III.	DAMPING DESIGN	11
A.	TEST STRUCTURE	11
B.	DAMPING TREATMENT LOCATION	11
C.	FREQUENCY, TEMPERATURE AND MATERIAL TYPES	18
D.	DAMPING TREATMENT THICKNESS	18
E.	MODAL STRAIN ENERGY ANALYSIS	27
IV.	EXPERIMENTS	31
A.	TESTING ARRANGEMENT	31
B.	TESTING PROCEDURE	32
1.	CASE WITH VISCOELASTIC MATERIAL ON OUTER SHELL	32
2.	CASE WITH VISCOELASTIC MATERIAL ON OUTER SHELL AND VANES	32
V.	RESULTS	36
A.	FREQUENCY RESPONSE MEASUREMENTS	36
1.	CASE WITH VISCOELASTIC MATERIAL ON OUTER SHELL	36
2.	CASE WITH VISCOELASTIC MATERIAL ON OUTER SHELL AND VANES	38
B.	COMPARISON WITH MODAL STRAIN ENERGY METHOD	38

C. STRUCTURAL DAMPING -----	39
D. DISCUSSIONS -----	39
VI. CONCLUSIONS -----	69
VII. RECOMMENDATIONS -----	70
APPENDIX A: INPUT DATA SETS FOR MSC/NASTRAN FOR UNDAMPED STRAIN ENERGY ANALYSIS AND FOR DAMPED MODAL STRAIN ENERGY(MSE) ANALYSIS -----	72
APPENDIX B: FORTRAN PROGRAM USED TO COMPUTE LOSS FACTORS FOR THREE LAYER SYSTEM -----	81
LIST OF REFERENCES -----	83
INITIAL DISTRIBUTION LIST -----	85

## **ACKNOWLEDGMENTS**

The author would like to extend sincere thanks to Prof. Young Shin and Dr. Kilsoo Kim for their guidance and assistance in the performance of this research. Additionally, the author would like to express gratitude to Mr. Tom McCord and Mr. Mardo Blanco for their excellent material and lab support. Finally, the author would like to acknowledge the support of Dr. P. Mahmoodi, Dr. D. Nelson and the personnel at the 3M Corporate Research Laboratories, Saint Paul, Minnesota, who provided material, background information and many valuable suggestions and comments in the conduct of this research.

## **I. INTRODUCTION**

### **A. BACKGROUND**

Modern high strength materials such as steel, aluminum and titanium are widely used in all areas of construction. However, these materials have very little inherent damping. Structures constructed of these materials are apt to experience large, unwanted resonant vibrations which can result in structural damage and the transmission of large amounts of noise to the environment. Most materials which have high inherent damping, such as viscoelastic materials, have very low load carrying capability, making them unsuitable for present day high strength applications. A combination of a high strength material with a material that has high inherent damping can exhibit the necessary strength/damping characteristics, if properly designed. One of the more effective methods of combining these materials is through the use of constrained viscoelastic layer damping treatments. Unfortunately, the proper design of constrained viscoelastic layer damping treatments for structures can be very difficult for a number of reasons, including the following:

- The material properties of viscoelastic materials vary greatly with temperature and frequency.
- Closed form equations which allow easy analytical solutions to design problems are only available for simple beams and plates.
- The amount of damping that can be obtained from a given constrained viscoelastic layer damping treatment is heavily dependent on the location of the treatment on the structure. Improper placement of the treatment on the structure will greatly mitigate the potential improvements in system damping.
- Until recently, the variation of viscoelastic material properties with frequency made finite element modeling a prohibitively costly way of

determining structural system damping due to the large CPU time requirements. This was especially so if an iterative design process was to be used, requiring analyses of many damping treatment combinations.

## B. PURPOSE

Recently, a new finite element analysis technique has been developed which is effective in modeling structures which use constrained viscoelastic layer damping treatments, and is cost effective enough to use with complicated structures. This technique, called the Modal Strain Energy (MSE) method, uses structural strain energy to approximate the damping properties of the structure with an applied damping treatment. The MSE method has been validated by comparison to classical frequency response finite element techniques and by experimentation for many simple structural geometries [Refs. 1,2]. The purposes of this study are to develop and apply a design procedure for constrained layer damping treatments for general, complicated plate and shell type structures, and to investigate the effectiveness of a constrained layer damping treatment for a typical plate and shell type structure. Experimental techniques are used to measure the vibrational amplitudes in the structure to determine the effectiveness of the constrained layer damping treatment, and to compare to the results obtained using the MSE method.

## II. THEORY

### A. EQUATIONS OF MOTION AND VIBRATION MODES

Continuous systems that exhibit only one principal vibrational mode (such as a spring and viscous damper with an attached mass) are said to have only one degree of freedom. The equation of motion for such systems is as follows: [Ref. 3]

$$m\ddot{x}(t) + c\dot{x}(t) + kx(t) = F(t) \quad (2.1)$$

where,

$x(t)$  = system displacement

$\dot{x}(t)$  = system velocity

$\ddot{x}(t)$  = system acceleration

$m$  = system mass

$c$  = system damping

$k$  = system stiffness

$F(t)$  = externally applied time varying force

The external force and resulting response can be assumed to be of the form:

$$F(t) = Fe^{j\omega t} \quad (2.2)$$

$$x(t) = Xe^{j\omega t} \quad (2.3)$$

where,

$F$  = force amplitude

$X$  = response amplitude

$\omega$  = frequency of harmonic load (radians/sec)

Substitution of the assumed force and response into the system equations of motion provides the solution for the displacement X:

$$\frac{X}{F} = \frac{1}{(k - m\omega^2) + j(c\omega)} \quad (2.4)$$

If the continuous system cannot be represented by only one degree of freedom, two options are available to describe the system's vibratory behavior. Closed form solutions to the equations of motion can be found for simple geometries such as beams and plates. If the system is more complicated than that, however, the system response can only be found by discretization of the equations of motion. In this case, the system is physically split into many small pieces whose motion is then solved for. The equations of motion for this case are as follows:

$$[M]\{\ddot{x}\} + [C]\{\dot{x}\} + [K]\{x\} = \{F(t)\} \quad (2.5)$$

where,

- $\{x\}$  = system displacement vector
- $\{\dot{x}\}$  = system velocity vector
- $\{\ddot{x}\}$  = system acceleration vector
- $[M]$  = system mass matrix
- $[C]$  = system damping matrix
- $[K]$  = system stiffness matrix
- $\{F(t)\}$  = externally applied load vector

The solution to this discretized form of the system equations of motion can be calculated by hand if the system can be adequately described by two or three degrees of freedom. For more complicated systems, however, the matrix operations become too complicated and must be solved using a digital computer.

Modal analysis involves the determination of system natural frequencies and mode shapes of vibration for each natural frequency. The natural frequencies and mode shapes are solved for as follows. First, the

applied force vector and damping matrix are set equal to zero. This leaves the equations of motion in the form:

$$[M]\{\ddot{x}\} + [K]\{x\} = 0 \quad (2.6)$$

This is a simple eigenvalue problem that is easily solved for the eigenvalues and eigenvectors. For the physical system being modeled, the eigenvalues will represent the system's natural frequencies, while the eigenvectors will represent the system's mode shapes. The system's equations of motion can be transformed into a set of uncoupled equations which can then be solved individually through the use of the following transformation equation:

$$\{x(t)\} = [\phi]\{\alpha(t)\} \quad (2.7)$$

where,

$\{\alpha(t)\}$  = principal or modal coordinate vector

$[\phi]$  = mode shape matrix

$\{x(t)\}$  = original displacement vector

Assuming that the damping matrix in equation (2.5) can be approximated through the use of an appropriate diagonal matrix, and using the following two relations:

$$\omega_n^2 = \frac{k}{m} \quad (2.8)$$

$$\zeta = \frac{c}{2\sqrt{km}} \quad (2.9)$$

a new system of individual uncoupled equations can be obtained [Ref. 2]:

$$\ddot{\alpha}_i(t) + 2\zeta_i \omega_i \dot{\alpha}_i(t) + \omega_i^2 \alpha_i(t) = \bar{f}_i(t) \quad (2.10)$$

where,

$\ddot{\alpha}_i(t)$  = modal acceleration for  $i^{th}$  mode

$\dot{\alpha}_i(t)$  = modal velocity for  $i^{th}$  mode

$\alpha_i(t)$  = modal displacement for  $i^{th}$  mode

$\zeta_i$  = critical damping ratio for  $i^{th}$  mode

$\omega_i$  =  $i^{th}$  natural frequency

$\bar{f}_i(t)$  = modal force for  $i^{th}$  mode

Since this system of equations is uncoupled, the equations are readily solved one at a time.

## B. VISCOELASTIC DAMPING

One of the effective means of controlling unwanted resonant vibrations is through the use of viscoelastic materials. Many different applications of viscoelastic damping have been developed including free layer viscoelastic damping treatments, constrained layer viscoelastic damping treatments, concentrated dampers, and others. Every specific application takes advantage of the viscoelastic material's unique ability to dissipate vibrational energy as heat through the stretching and relaxation of long polymeric molecule chains [Ref. 4]. Since the material dissipates energy through the stretching and relaxation of its molecules, anything that affects the ability of the molecules to move will affect the damping capability of the material. Thus, the material properties of viscoelastic materials, especially shear modulus and loss factor, vary considerably with vibration frequency and temperature. The shear modulus is one third of the storage (Young's) modulus, while loss factor is defined as twice the critical

damping ratio. A plot of storage modulus and loss factor vs frequency for viscoelastic materials is shown in Figure 2.1 [Ref. 4].

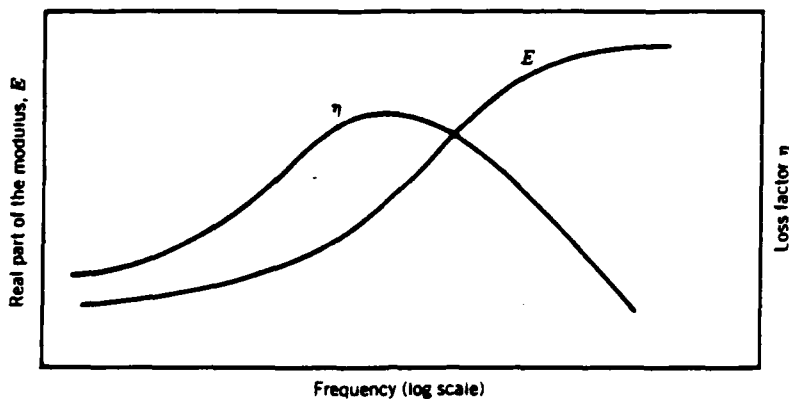


Figure 2.1. Variation of viscoelastic material properties with frequency [Ref. 4].

Note that the storage modulus rises with increasing frequency, while loss factor rises and then falls. A plot of storage modulus and loss factor vs temperature for viscoelastic materials is shown in Figure 2.2 [Ref. 4].

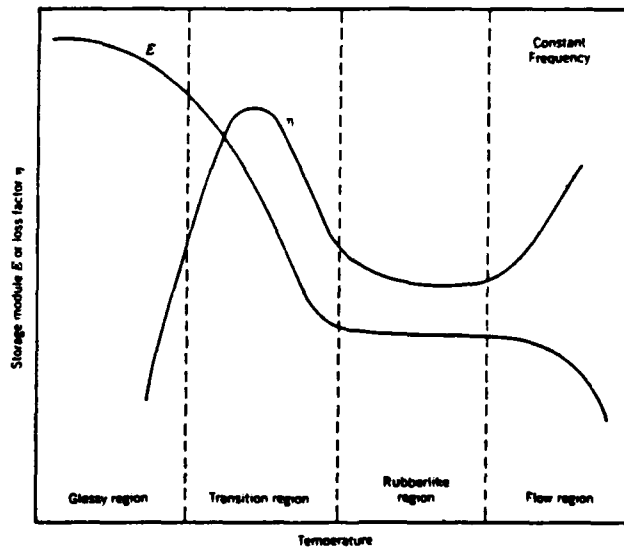


Figure 2.2. Variation of viscoelastic material properties with temperature [Ref. 4].

Note that storage modulus generally drops as temperature increases, while the loss factor rises and falls. The transition region is the most important region for most damping applications, since loss factor peaks and the storage modulus is high enough to allow good resistance to shearing.

One of the more effective methods of using viscoelastic materials is through the use of a constrained viscoelastic layer damping treatment. In this application, the system to be damped is covered, either totally or partially, with a layer of viscoelastic material followed by a layer of some constraining material, as shown in Figure 2.3.

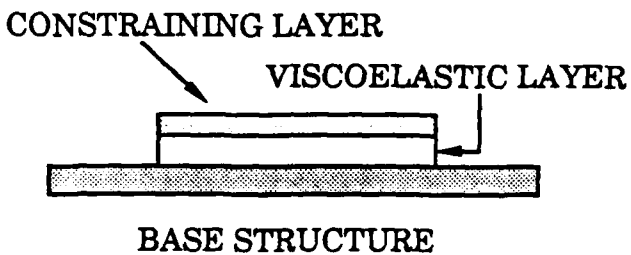


Figure 2.3. Constrained layer damping treatment.

As the structure deforms the constraining layer prevents movement of the upper portion of the viscoelastic material. At the same time, the lower portion of the viscoelastic material is forced to move with the base structure. Thus, the viscoelastic layer is placed into shear, with the shearing action stretching the molecules of the viscoelastic material and causing dissipation of vibrational energy. Since the shearing action in the viscoelastic material is so great, bending deformations in the viscoelastic

material layer can be neglected. In this case, the energy dissipation in the viscoelastic layer is given by the following expression [Ref. 4]:

$$D_s = \pi \int_{\text{vol}} \eta E \gamma^2 dV \quad (2.11)$$

Most significantly, the amount of energy dissipated in the viscoelastic material layer is proportional to the square of the shear strain. Thus, the location of the damping treatment on the structure is the single most important factor in designing an appropriate constrained viscoelastic layer damping treatment. Also, of course, the energy dissipation is dependent on the material properties of the viscoelastic material, which themselves are dependent on frequency and temperature. Finally, since the energy dissipation integral is taken over the viscoelastic material volume, the area and thickness of the constrained layer damping treatment will influence the amount of energy dissipation realized.

### C. MODAL STRAIN ENERGY METHOD

Most complicated structures can be adequately analyzed through the use of finite element techniques. Unfortunately, finding the frequency response of a structure whose material properties change with frequency has been extremely time consuming and costly, since many individual runs must be made with the material properties changing at each frequency increment [Ref. 1]. Add to this the necessity to try different design options depending on the specific design requirements, and finite element analysis can be too great of an expense. The recent development of the Modal Strain Energy (MSE) method, however, makes finite element analysis for even the most complicated structures an analysis and design possibility [Ref. 5].

Central to the MSE method is the idea that the structure's damped mode shapes and natural frequencies can be adequately approximated by the undamped mode shapes and natural frequencies of the structure [Ref. 1]. Thus, costly complex eigenvalue analysis is completely avoided. The first step is to find the mode shapes and natural frequencies of the structure by

conducting a finite element modal analysis. Also, the amount of strain energy in each element of the finite element model is determined. It can be shown [Ref. 1] that the modal loss factor can be approximated by the following expression:

$$\eta_i = \eta_{v,i} \left( \frac{V_{v,i}}{V_{T,i}} \right) \quad (2.12)$$

where,

$i$  = mode number

$\eta_i$  = modal loss factor

$\eta_{v,i}$  = viscoelastic material loss factor

$V_{v,i}$  = strain energy in viscoelastic material for  $i^{\text{th}}$  mode

$V_{T,i}$  = strain energy in total structure for  $i^{\text{th}}$  mode

Since  $\eta=2\zeta$  this expression can be readily substituted into equation (2.10). Also, since the modal analysis gives the system's natural frequencies and mode shapes, all of the constant values of equation (2.10) have been found, and the equations of motion can now be solved.

### **III. DAMPING DESIGN**

#### **A. TEST STRUCTURE**

The test structure used for this design procedure was a set of two concentric cylindrical shells connected by four vanes as shown in Figure 3.1. This structure had previously been used to investigate the ability of bolted connections to dissipate vibrational energy and thereby increase structural damping [Refs. 6,7]. This structure was useful because it was a structure typical of those with very little inherent damping. A constrained layer damping treatment was chosen for application in an attempt to reduce the large resonant vibrations that this structure experienced [Ref. 6,7]. The following variables were considered in designing the proper constrained layer damping treatment:

- Damping treatment location on the structure.
- Temperature and frequency range of interest.
- Material type for the viscoelastic and constraining layers.
- Area and thickness of the viscoelastic and constraining layers.

#### **B. DAMPING TREATMENT LOCATION**

The first step in designing a proper damping treatment was to determine where to place it on the structure. From equation (2.11), it was clear that locations that would provide high shear strains in the damping material would be the best candidates for a damping treatment application.

The first method of determining which areas would provide high shear strains in the damping material involved visual observation of the mode shapes of the test structure. Iverson experimentally determined the first eight mode shapes of vibration during his joint damping investigation using a Hewlett Packard 5451C Fourier Analyzer [Ref. 6]. Figures 3.2 and 3.3 show the first two mode shapes of the eight that were determined. Table 3.1 shows the results of this visual mode shape investigation, with a one



**Figure 3.1. The test structure.**

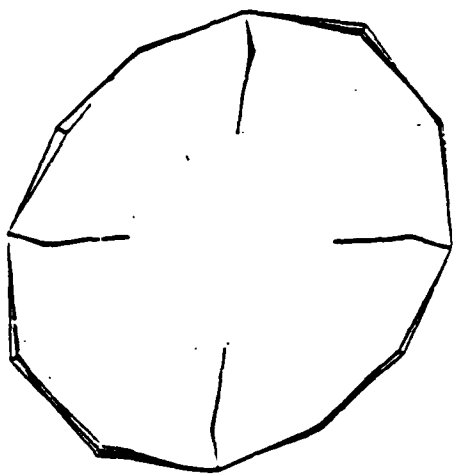


Figure 3.2. First mode shape of vibration of the test structure. [Ref. 6]

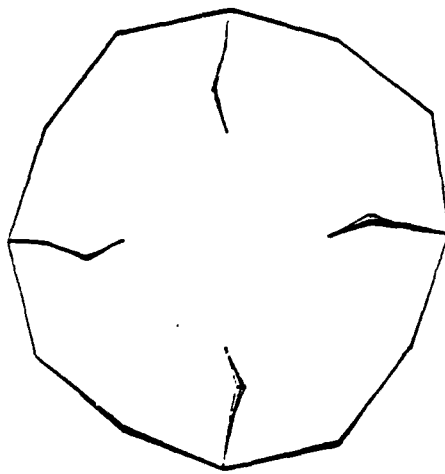


Figure 3.3. Second mode shape of vibration of the test structure. [Ref. 6]

denoting a large amount of motion in a given area, and a zero denoting little or no motion in that area for each mode. As Table 3.1 shows,

**TABLE 3.1. VISUAL MODE SHAPE INVESTIGATION.** (A "1" indicates a large amount of motion for that location for that mode. A "0" indicates little or no motion.)

MODE	OUTER SHELL	INNER SHELL	VANE	BOLTED JOINT
1	1	1	0	1
2	0	1	1	0
3	1	0	1	0
4	1	0	0	0
5	1	0	1	0
6	1	0	1	0
7	1	0	0	1
8	1	0	0	0
TOTAL	7	2	4	2

most of the structural motion took place in the outer shell area, with a moderate amount of motion taking place in the vanes. Almost no motion occurred at the vane connections to the outer or inner shells. Visual observation of the animated mode shapes as seen on the HP 1347A display terminal reinforced these conclusions. Almost every mode analyzed showed sizeable deformations in the outer shell. Some modes showed almost no vane deformation, such as modes 1,4,7, and 8. In summary, investigation of the mode shapes indicated that the outer shell was a primary candidate for damping treatment application, with the vanes as a possible secondary candidate.

The second method of determining damping treatment location was through the use of strain energy distribution data [Ref. 1]. In its simplest

definition, strain energy is the work required to deform an elastic body. For a rod in tension this is [Ref. 8]:

$$U = \frac{1}{2} V E \epsilon_{xx}^2 \quad (3.1)$$

where,

$U$  = strain energy

$E$  = Young's Modulus

$\epsilon_{xx}$  = elastic strain

$V$  = volume

Thus, strain energy, like the energy dissipation of equation (2.11), is proportional to the square of the deformation of the object in question. Thus, any area of the test structure that had a high strain energy was a likely candidate for a constrained layer damping treatment since bending deformations in the structure would lead to shear deformations in the viscoelastic material due to the constraining layer. To determine the strain energy distribution in the structure, a finite element model of the undamped structure was constructed using MSC/NASTRAN. To model this structure adequately, a finite element model consisting of 128 grid points and 108 shell elements was constructed as shown in Figures 3.4 and 3.5. CQUAD4 shell elements were used to model the structure. A cylindrical coordinate system was used instead of the default rectangular coordinate system to make grid point location definition easier. The grid points were numbered as shown. A modal analysis was run, with strain energy for each element for each mode selected as output. The MSC/NASTRAN code for this strain energy run is included in Appendix A.

The results of the strain energy run are shown in Table 3.2. The strain energies are given in percent of the total structural strain energy for each mode. The "inner vane" elements were the vane elements closest to the inner shell. The "outer vane" elements were the vane elements closest to the outer shell. The "side outer shell" elements were the outer shell

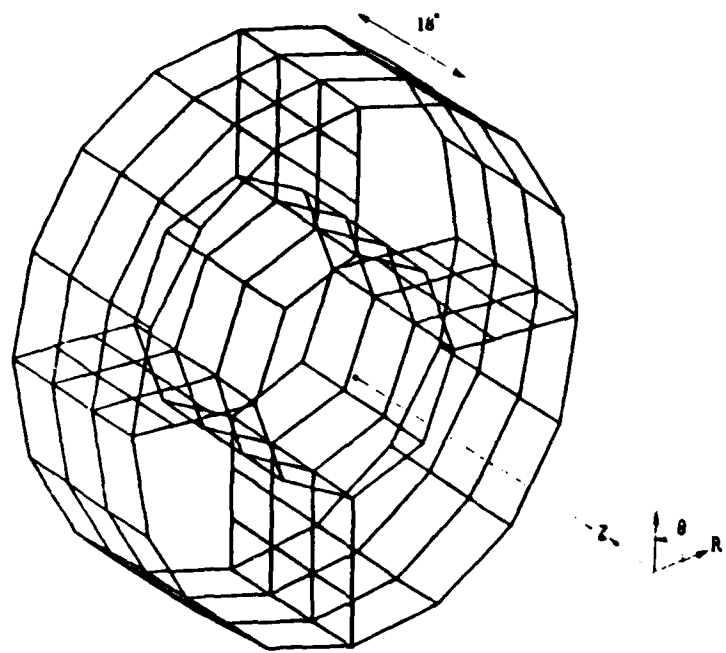
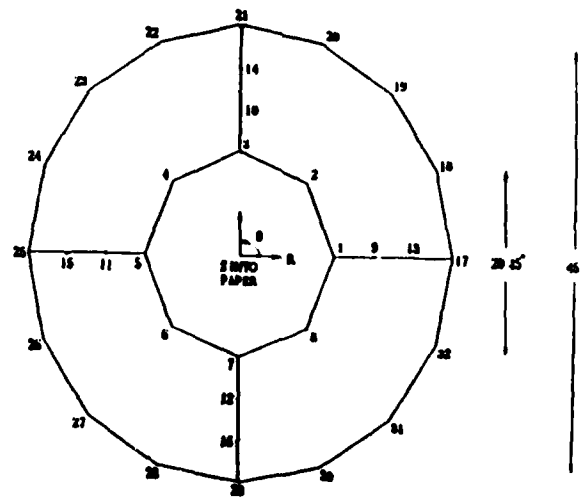


Figure 3.4. MSC/NASTRAN finite element model of test structure.



**Figure 3.5. MSC/NASTRAN finite element model of test structure (front view).**

elements closest to the vanes. The data showed that the outer shell was the most likely candidate for a damping treatment. The data also showed that the vanes were possible secondary candidates for damping treatments. The inner shell was confirmed to be an area of very low strain energy and was thus determined to be a poor candidate for a damping treatment. Also, for both the vanes and the shells, the elements closest to the bolted connections gave the highest strain energy. This was interesting since the

TABLE 3.2. STRAIN ENERGY DISTRIBUTION IN UNDAMPED  
STRUCTURE DETERMINED BY  
MSC/NASTRAN FINITE ELEMENT ANALYSIS.

MODE	INNER SHELL	INNER VANE	MIDDLE VANE	OUTER VANE	SIDE OUTER SHELL	MIDDLE OUTER SHELL
1	2.438	18.109	3.437	37.721	9.325	28.705
2	0.464	10.464	6.639	18.662	38.692	25.079
3	3.758	52.926	8.302	11.222	17.761	6.032
4	2.384	15.704	1.911	22.105	31.191	26.751
5	2.119	15.841	1.900	22.155	31.179	26.793
6	88.230	0.169	0.063	0.045	4.968	6.526
7	0.720	6.986	2.405	15.929	32.224	41.704
8	2.477	1.306	1.646	4.266	46.772	43.444
TOTAL	102.59	121.60	26.303	132.11	212.11	205.03
AVG/MODE	12.82	15.20	3.29	16.51	26.51	25.63

experimental mode shapes showed the connections between the vanes and the shells to be an area of little deformation. However, since the area near the connections is a transition area between an area of little deformation and an area of large deformation, large bending stresses are likely (similar

to a cantilever beam near the rigid wall), causing this area to have a high strain energy.

### C. FREQUENCY, TEMPERATURE AND MATERIAL TYPES

The next step in the design process was the determination of the applicable temperature and frequency ranges, and the material types for the viscoelastic and constraining layers.

The temperature for all design work was considered to be 70°F. Although some small temperature fluctuations occurred during experimentation, this temperature was a good average value for use in analytical design work. The frequency range of interest was 0 to 300 Hz. This low frequency range was chosen since the absorption of sound in seawater rises as the square of frequency as shown by the following equation [Ref. 9]:

$$a = 6.8f^2 \times 10^{-5} \text{ dB / yard} \quad (3.2)$$

where,

a = absorption of sound in seawater at 65°F

f = frequency of sound waves

Thus, sound created by low frequency vibrations is not easily absorbed in seawater and must be prevented through the dissipation of structural vibration energy.

The viscoelastic layer material chosen was 3M ISD-112 since it displays a very high loss factor in the frequency range of interest. Aluminum was chosen for the constraining layer since it is light, relatively stiff, easy to fabricate, and is commonly used in most constrained layer damping treatments.

### D. DAMPING TREATMENT THICKNESS

To complete the initial damping treatment design, only the thicknesses were left to be determined. To accomplish this, subsystem analysis was performed. To do this the structure was broken down into smaller subsections, and the damping design was conducted for these

smaller subsections. Numerous methods had been suggested for accomplishing this subsystem analysis. The system's dimensions could be matched to a beam or plate, and then the "effective thickness" could be adjusted to make the natural frequencies match [Ref.4 ]. An alternative was to insure that the node line distances for the mode of interest matched the wavelength of vibration of the beam or plate approximation [Ref. 10]. Finally, simply matching the boundary conditions of the subsystem with the boundary conditions of a beam or plate had shown reasonable accuracy [Ref.11].

The test structure's first mode shape, corresponding to the first natural frequency of 29.7 Hz is shown in Figure 3.2. From this first mode shape, and from close observation of the animated first mode shape, it was clear that for the first mode of vibration the outer shell flexed back and forth as shown in Figure 3.6. Thus, each quarter of the outer shell behaved roughly like the first mode of a curved beam with simply supported ends. The equations for the system loss factor for a simply supported beam were therefore used to approximately predict system damping for the first mode of vibration with one quarter of the outer shell used as the subsystem.

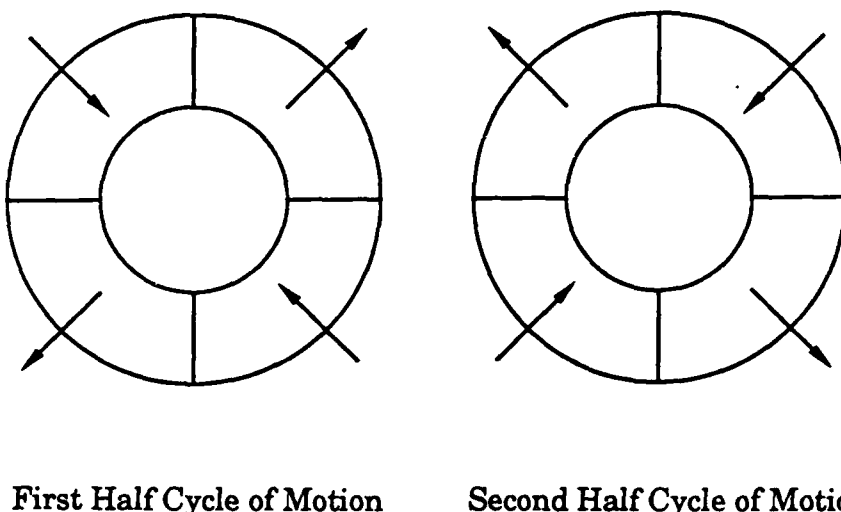


Figure 3.6. Motion of test structure during first (29.7 Hz) mode of vibration.

For a three layer system of the type shown in Figure 3.7, which is typical of a constrained layer damping treatment, the flexural rigidity can be expressed in closed form by: [Ref. 12]

$$EI = \frac{E_1 H_1^3}{12} + \frac{E_2 H_2^3}{12} + \frac{E_3 H_3^3}{12} + E_1 H_1 D^2 + E_2 H_2 [H_{21} - D]^2 + E_3 H_3 [H_{31} - D]^2 \\ - \left\{ \frac{E_2 H_2^2}{12} + \frac{E_2 H_2}{2} (H_{21} - D) + E_3 H_3 [H_{31} - D] \right\} \frac{[H_{31} - D]}{[1 + g]} \quad (3.3)$$

where,

$$D = \frac{E_2 H_2 [H_{21} - \frac{H_{31}}{2}] + g[E_2 H_2 H_{21} + E_3 H_3 H_{31}]}{E_1 H_1 + \frac{E_2 H_2^2}{2} + g[E_1 H_1 + E_2 H_2 + E_3 H_3]} \quad (3.4)$$

$$H_{21} = \frac{H_1 + H_2}{2} \quad (3.5)$$

$$H_{31} = \frac{H_1 + 2H_2 + H_3}{2} \quad (3.6)$$

$$g = \frac{G_2}{E_3 H_2 H_3 K^2} \quad (3.7)$$

where,

**H** = section thickness

**E** = Young's Modulus

**G** = shear modulus

**I** = area moment of inertia

**K**<sup>2</sup> = wave number

and,

Subscript 1 refers to the base structure

Subscript 2 refers to the viscoelastic layer

Subscript 3 refers to the constraining layer

No subscript refers to the composite structure

The wave number is different depending on the type of three layer structure. For a simply supported beam it is computed as follows:

$$K_n^2 = \left( \frac{n\pi}{L} \right)^2 \quad (3.8)$$

where,

n = mode number

L = length of beam

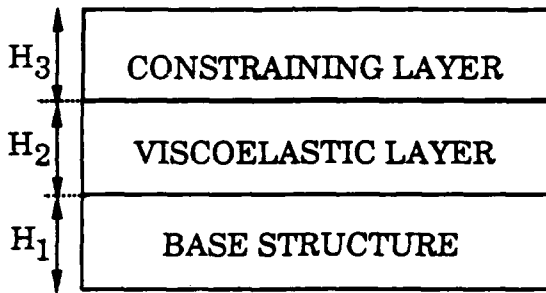


Figure 3.7. Constrained viscoelastic layer damping treatment.

The preceding equations were used to determine the loss factor and shear modulus for the subsystem with a constrained layer damping treatment. The following inputs to these equations were used:

- $H_1 = 0.25$  in.
- $E_1 = 30 \times 10^6$  PSI
- $E_3 = 10 \times 10^6$  PSI
- $L = \text{Circumference}/4 = (\pi d)/4 = (\pi * 45 \text{ in.})/4 = 35.3 \text{ in.}$

- $n = 1$
- $G_2, \eta_2$  = found from material property graph
- $H_2, H_3$  = varied by designer to find optimum values

The material property values for 3M ISD-112 were displayed on a reduced frequency nomograph as shown in Figure 3.8. To find the material properties of the viscoelastic material, simply move across the graph from the right at the proper frequency, and move down along the constant temperature line until the two lines intersect. Then draw a vertical line. The intersection of this vertical line with the two material property curves gave the desired values for the given frequency and temperature. Thus, the values for  $H_2$  and  $H_3$  were the only variable inputs to the equations for system damping and system loss factor. These thickness values were varied and loss factor curves for each combination were plotted. A FORTRAN program shown in Appendix B was written to solve the system loss factor equations for each combination of  $H_2$  and  $H_3$ . The damping material thickness,  $H_2$ , was held constant at 0.005 in. while the constraining layer thickness,  $H_3$ , was varied through eight different values from 0.005 in. to 0.040 in., resulting in eight system loss factor curves on one plot for a constant  $H_2$  of 0.005 in. [Ref. 13]. Then, the damping material thickness  $H_2$  was changed from 0.005 in. to 0.040 in. in increments of 0.005 in., with a new graph plotted at each increment. The curves for  $H_2 = 0.005$  in.,  $H_2 = 0.030$  in. and  $H_2 = 0.040$  in. are shown in Figures 3.9 through 3.11. Generally, as  $H_3$  increased, the loss factor increased for constant  $H_2$ . Also, as  $H_2$  increased for a constant  $H_3$ , the loss factor increased. The loss factor curves show that as  $H_2$  approached 0.040 in., the curves became very peaky and the curves maximum points shifted radically to lower temperatures. Also, low values of  $H_2$  and  $H_3$  did not provide adequate levels of damping. Therefore, values of 0.030 in for  $H_2$  and 0.040 in for  $H_3$  were chosen as final design values. At a temperature of 70°F, this combination provided a theoretical system loss factor of 0.087.

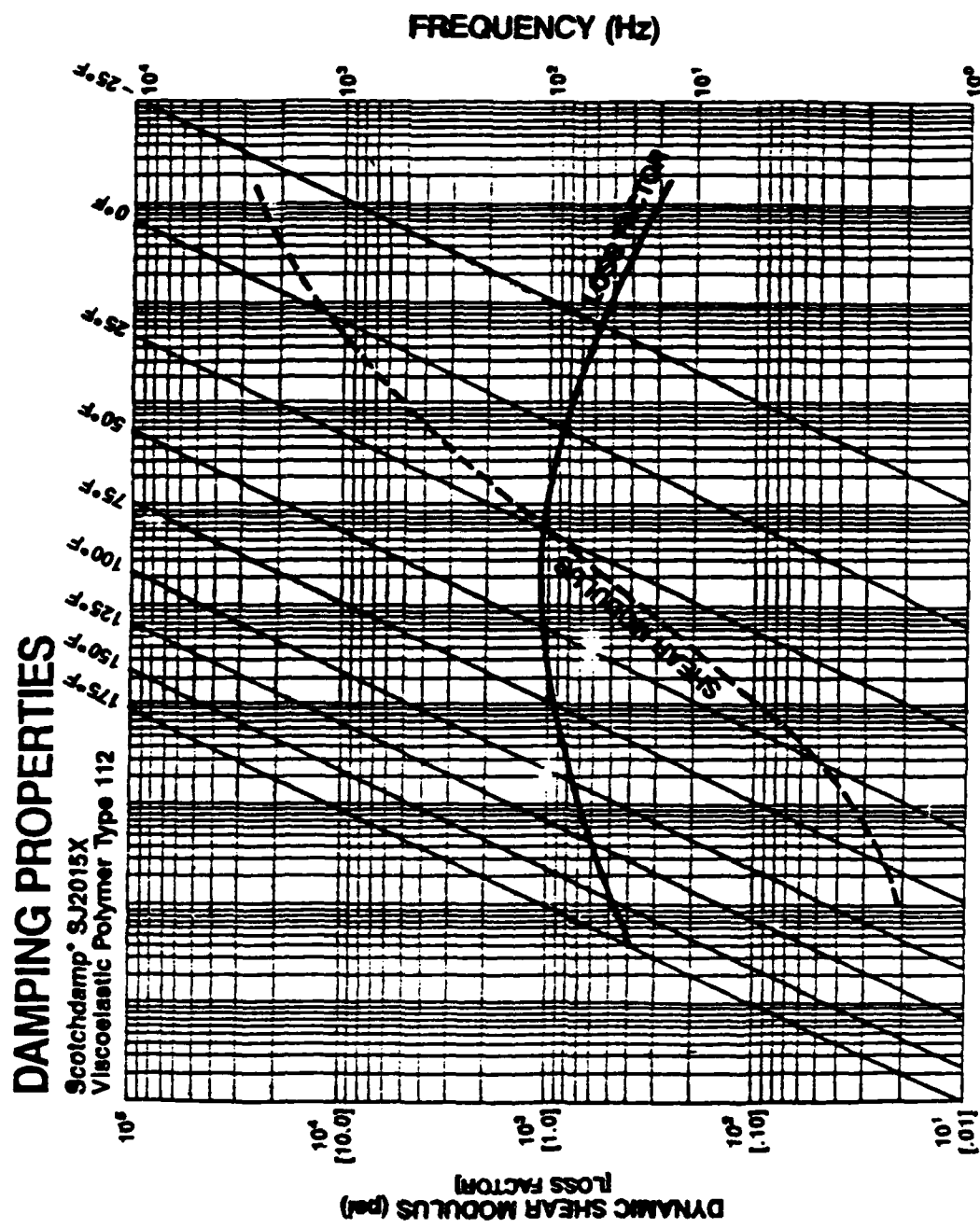


Figure 3.8. Reduced frequency nomograph for 3M ISD-112.

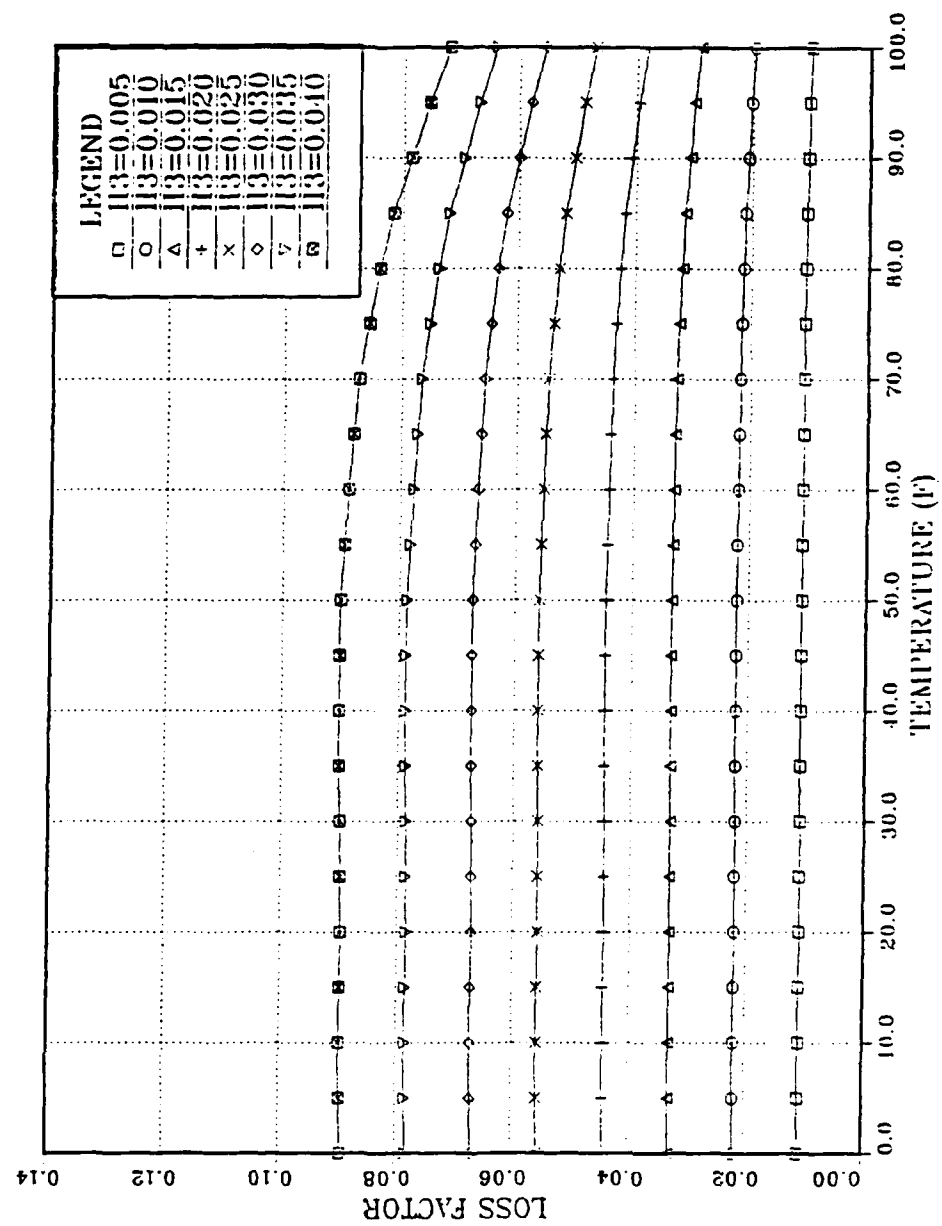


Figure 3.9. System loss factor vs. temperature for  $H_2 = 0.005$  in,  
frequency is constant at 29.7 Hz.

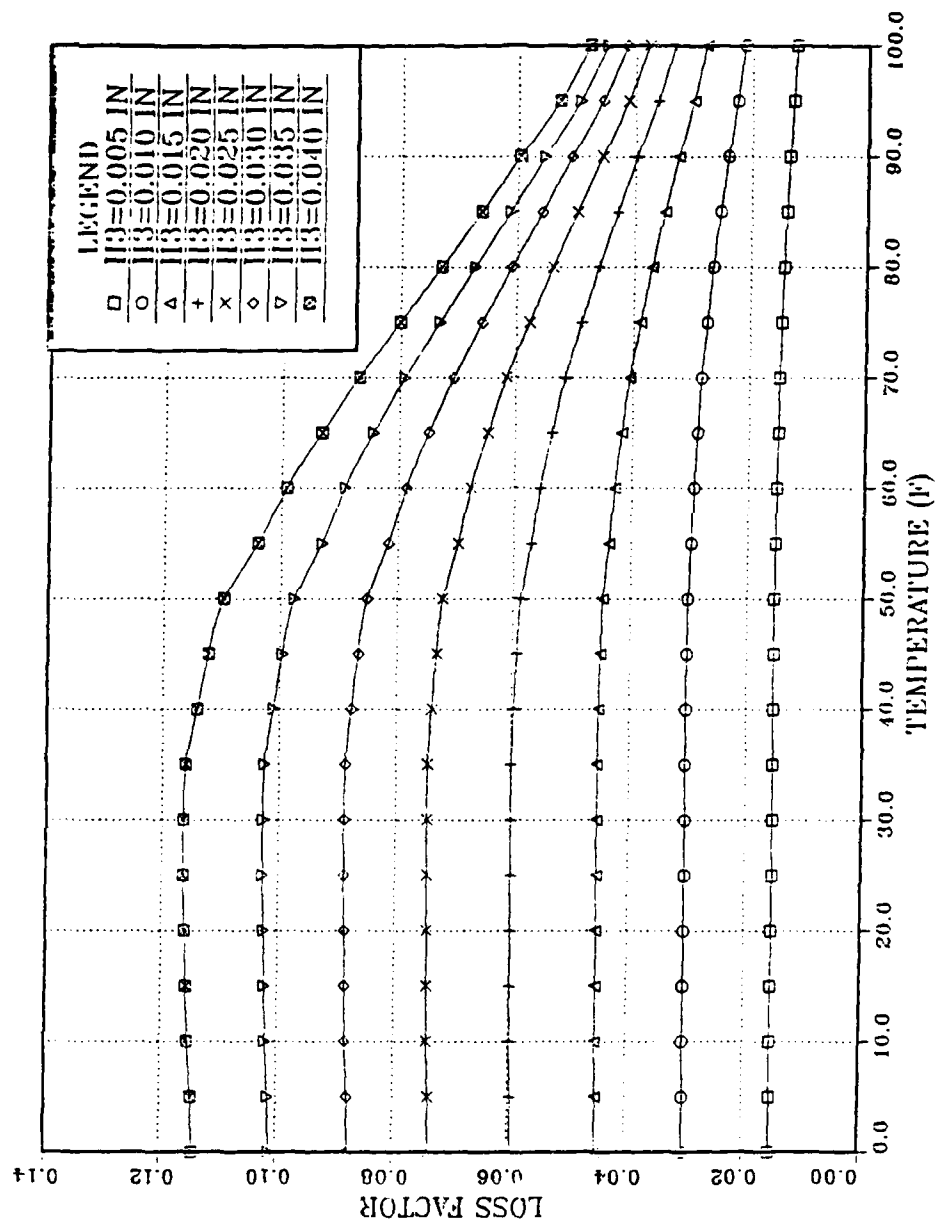


Figure 3.10. System loss factor vs. temperature for  $H_2 = 0.030$  in,  
frequency is constant at 29.7 Hz.

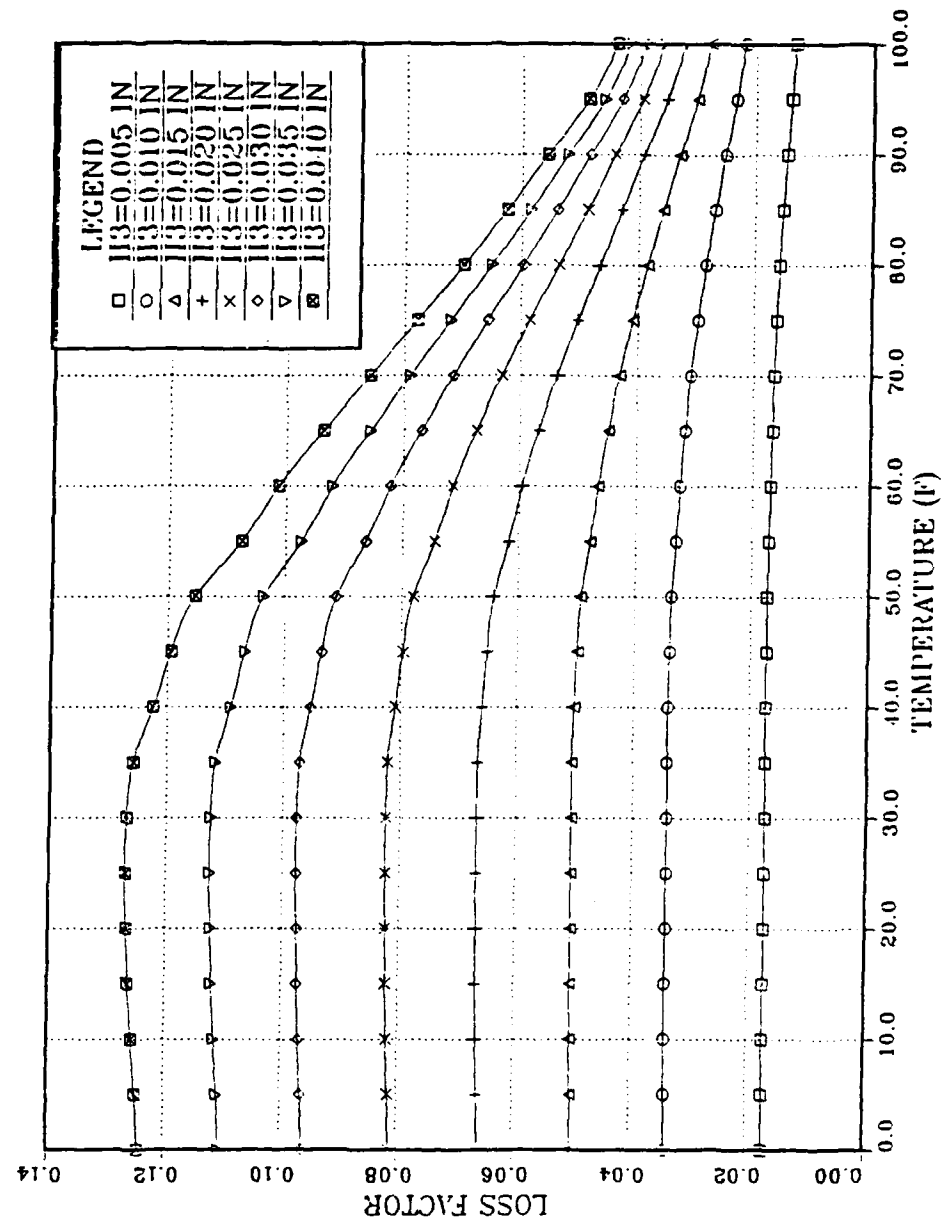


Figure 3.11. System loss factor vs. temperature for  $H_2 = 0.040$  in,  
frequency is constant at 29.7 Hz.

### E. MODAL STRAIN ENERGY ANALYSIS

To construct the modal strain energy finite element model, the model used for the undamped case was modified to include the addition of a 0.030 in. viscoelastic layer and a 0.040 in. constraining layer to the outer shell. The outer shell elements were offset toward the center of the structure by 0.125 in., and a second layer of grid points was placed 0.030 in. outside the first layer. Then, the viscoelastic layer was modeled using CHEXA elements, while the constraining layer was modeled using CQUAD4 elements and offset 0.020 in. away from the center of the structure, as shown in Figure 3.12.

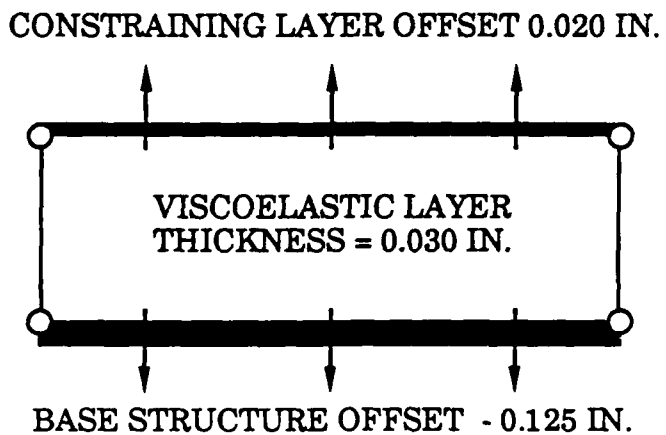


Figure 3.12. MSC/NASTRAN finite element model  
of constrained layer damping treatment.

A modal summation was performed as in [Ref. 2] using the following solution to equation (2.7):

$$X(\omega) = \frac{\phi_{E,i} \phi_{R,i} L / \omega_i^2}{\sqrt{\left\{1 - \left(\frac{\omega}{\omega_i}\right)^2\right\}^2 + \left\{\eta_{v,i} \left(\frac{V_{v,i}}{V_{t,i}}\right) \left(\frac{\omega}{\omega_i}\right)\right\}^2}} \quad (3.9)$$

where:

- $X(\omega)$  = amplitude of response as a function of frequency
- $\omega_i$  =  $i^{th}$  natural circular frequency
- $\phi_{E,i}$  = mode shape value for excitation grid point at  $i^{th}$  natural frequency
- $\phi_{R,i}$  = mode shape value for response grid point at  $i^{th}$  natural frequency
- $\eta_{v,i}$  = viscoelastic material loss factor
- $V_{v,i}$  = strain energy in viscoelastic material at  $i^{th}$  natural frequency
- $V_{t,i}$  = total strain energy in structure at  $i^{th}$  natural frequency
- $L$  = magnitude of load applied at excitation grid point

The loss factor in equation (3.9) is an iterated loss factor. Since it changes with frequency over the frequency range of interest, it must be adjusted for each natural frequency in the modal summation [Refs. 1,2]. The adjustment procedure was carried out as follows. Three finite element modal analysis runs were made with three different values of shear modulus for the viscoelastic material. This yielded three different natural frequencies for each mode, since increasing the shear modulus of the viscoelastic material increased the stiffness of the structure. These values

of shear modulus were added to a plot of shear modulus vs. frequency as shown in Figure 3.13. The three shear modulus values were then connected, and where the two lines intersected was where the shear modulus value was taken. Then, that shear modulus value was used to find the new loss factor value from the reduced frequency nomograph, Figure 3.8. Finally, this loss factor value was adjusted as follows:

$$\eta_i = \eta_{ic} \sqrt{\frac{G_{2,i}}{G_{2,REF}}} \quad 3.10$$

where,

$G_{2,REF}$  = shear modulus of viscoelastic material at 150 Hz

$G_{2,i}$  = shear modulus of viscoelastic material at  $i^{\text{th}}$  natural frequency

$\eta_{ic}$  = loss factor of viscoelastic material from reduced frequency nomograph

This most accurately described the true value of loss factor [Ref. 1].

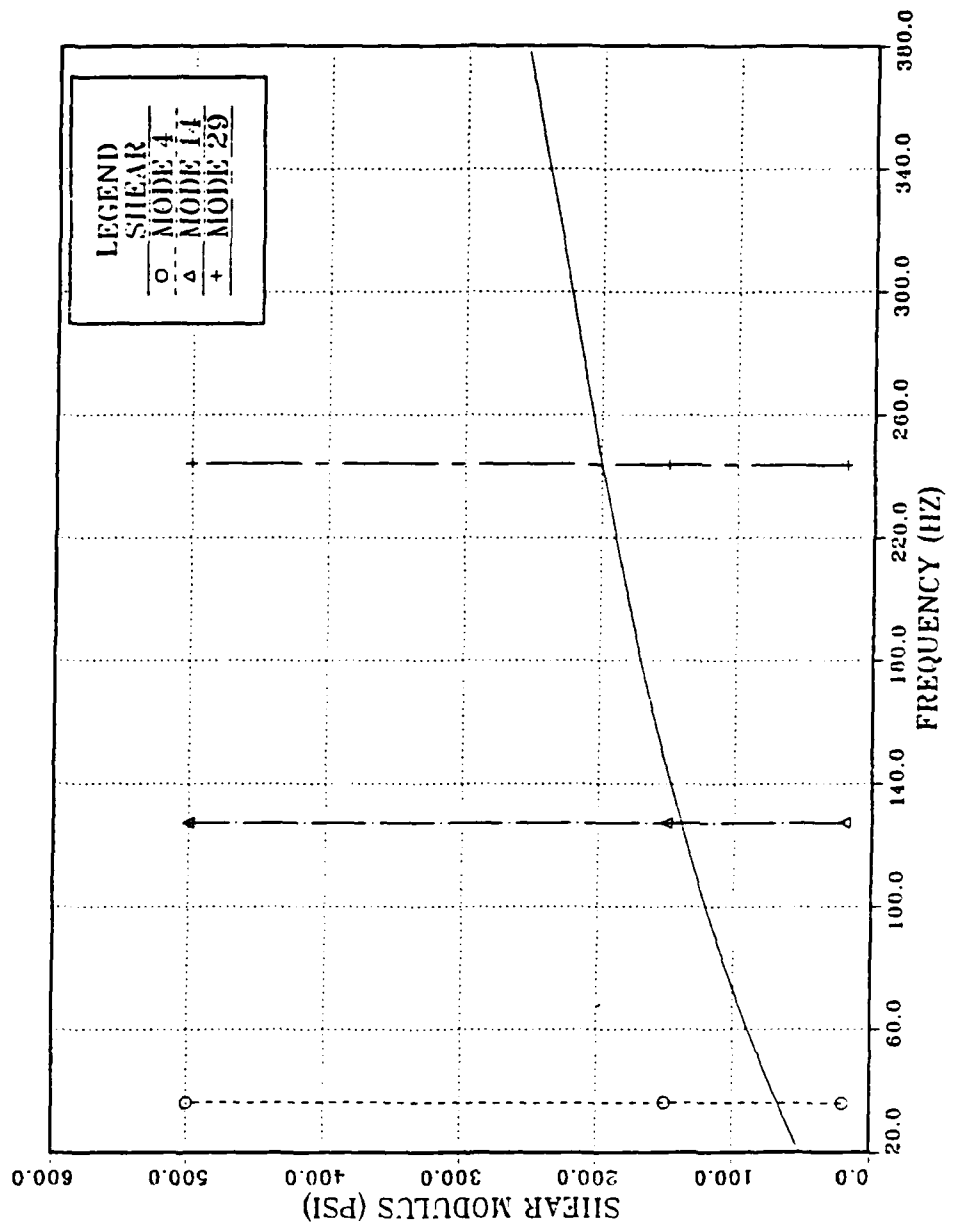


**Figure 3.13.** Shear modulus graphical iteration procedure for modes 4, 14 and 29. Value for shear modulus is chosen at intersection of two curves for each mode.

## IV. EXPERIMENTS

### A. TESTING ARRANGEMENT

The testing arrangement is shown in Figure 4.1. The user interface was provided by the Hewlett Packard(HP) 3562A Dynamic Signal Analyzer. The HP-3562A provided the source signals for the vibration generator, and analyzed the incoming input force signals and output acceleration signals. The HP-3562A was used to compute the frequency response, coherence, input power spectrum and output power spectrum using the discrete Fourier Transform at individual frequencies in the swept sine mode. Ten averages were used at each data point to provide good coherence measurements. Once data taking was complete for a given run, the data was saved on disk for later analysis.

Source signals from the HP-3562A were fed through a Wilcoxon Power Amplifier and split by a Wilcoxon Matching Network to power both the low frequency magnetic unit and the high frequency piezoelectric unit in the Wilcoxon F4/F7 vibration generator. The vibration generator was mounted 12 inches from the front and four inches from the inner shell of the test structure. The vibration generator was mounted inside a waterproof container since earlier research had required the immersion of the test structure in water. An integral force transducer was included in the base of the vibration generator to measure the input force. This input force signal was then fed through a PCB Corporation charge amplifier back to the HP-3562A. Two Endevco accelerometers were mounted on the test structure to measure system output acceleration. One accelerometer was located on the inside of the outer shell of the test structure, four inches from the front and twelve inches up from the vane. The other accelerometer was located four inches from the front and eight inches from the inner shell on the vane of the test structure. One of these output acceleration signals at a time could be fed through an Endevco signal conditioner back to the HP-3562A. Thus, the HP-3562A provided the source signal, measured input

force and output acceleration, computed and displayed the system frequency response, and then saved the data for future reference.

## B. TESTING PROCEDURE

### 1. Case With Viscoelastic Material on Outer Shell

The first series of tests was conducted with viscoelastic material on the outer shell of the test structure, with one constrained layer damping treatment located on each quadrant of the outer shell. Prior to application of the constrained layer damping treatment, baseline measurements with no damping treatment applied were taken for comparison purposes. Then the constrained layer damping treatment was applied carefully to prevent the entrapment of air between the viscoelastic material and the test structure. The constrained layer damping treatment was 18 inches wide, covering the entire width of the shell, and 27 inches long, covering most of the area between the area of the bolts as shown in Figure 4.2. Seven distinct frequency bands were used, including three wide range frequency bands, and four narrow range frequency bands. The three wide range frequency bands covered 15 to 115 Hz, 100 to 200 Hz and 200 to 300 Hz. The four narrow frequency bands covered 25 to 45 Hz, 95 to 115 Hz, 120 to 140 Hz, and 230 to 270 Hz. The narrow frequency bands were used to "zoom" in on natural frequencies of interest to provide higher resolution data at these critical areas. Measurements were taken using both the outer shell and vane accelerometers.

### 2. Case with Viscoelastic Material on Outer Shell and Vanes

The second series of tests was conducted with viscoelastic material applied to both the outer shell and the vanes of the test structure. Care was again taken when applying the viscoelastic material. The damping treatment was again 18 inches wide, covering the entire width of the vane, and nine inches long, covering almost the entire distance from the inner shell to the outer shell. The same frequency bands were used to

**facilitate comparison between the baseline, outer shell and outer shell/vane cases.**

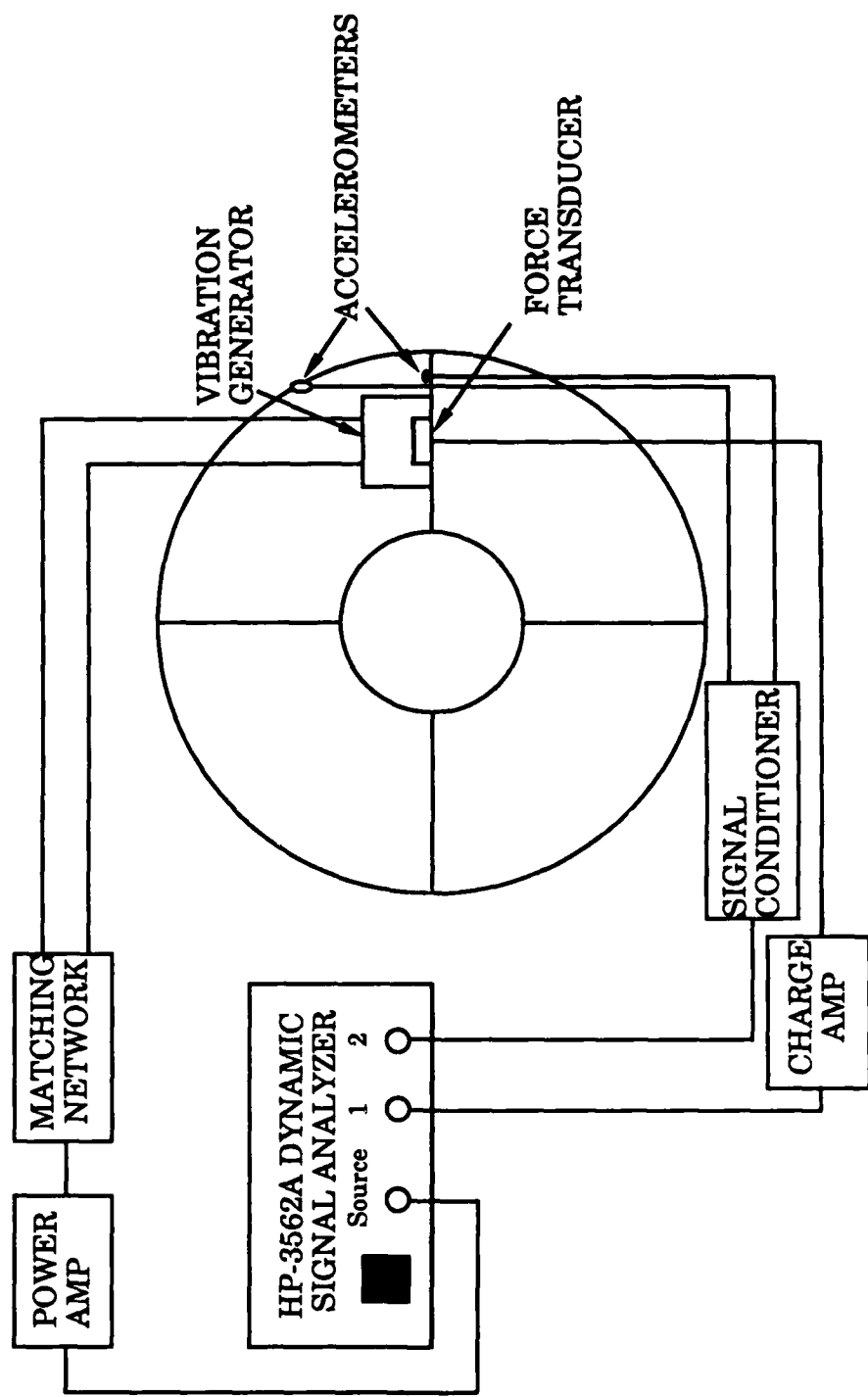
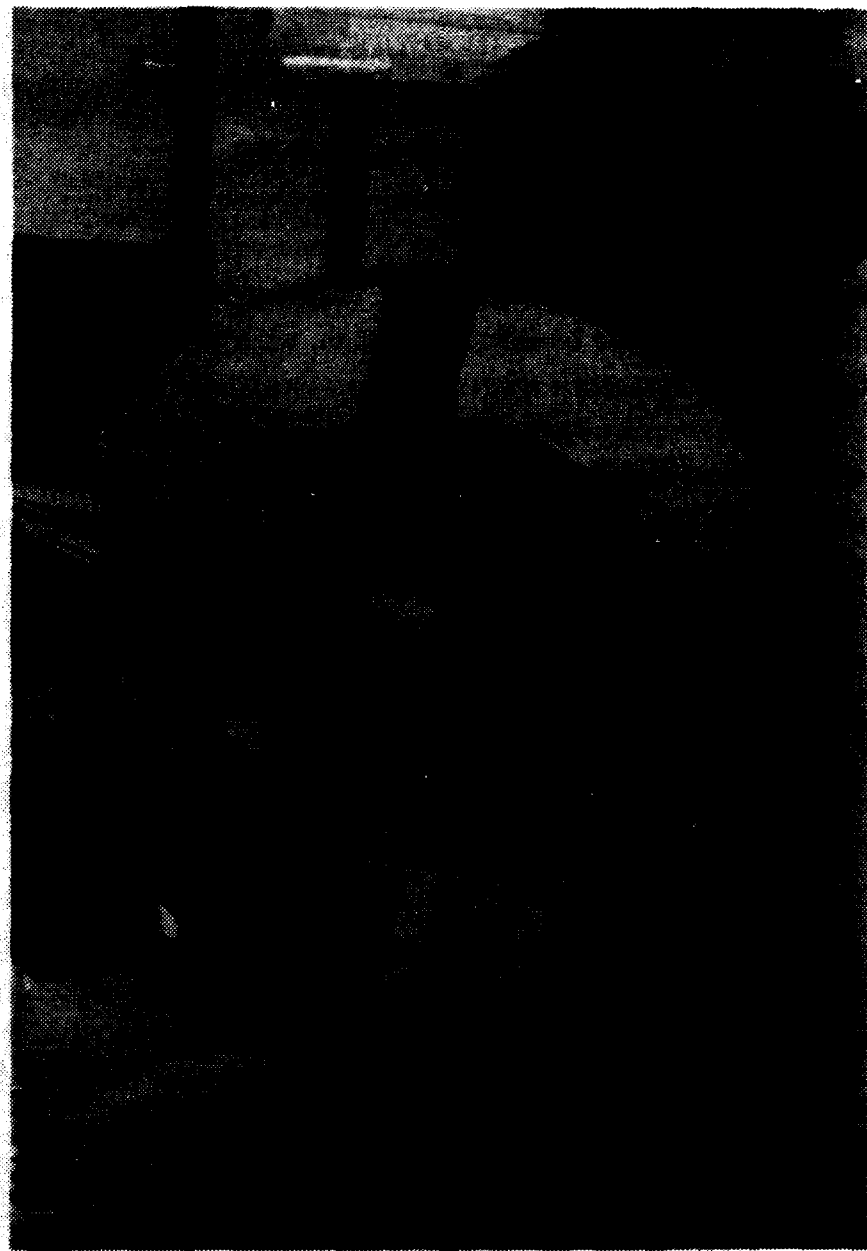


Figure 4.1. Testing arrangement.



**Figure 4.2. Location of viscoelastic material on outer shell.**

## V. RESULTS

### A. FREQUENCY RESPONSE MEASUREMENTS

#### 1. Case with Viscoelastic Material on Outer Shell

The frequency responses for the case with viscoelastic material on the outer shell are shown in Figures 5.1 through 5.9. In each case the dashed curve represents the baseline condition, with the solid line representing the test structure after damping treatment application. Also, each figure displays amplitude in dB, with 12.5 dB per division on the vertical axis, and measurements for Figures 5.1 through 5.7 were taken on the outer shell of the test structure. The frequency response of the test structure for the 15 to 115 Hz range for both the baseline and viscoelastic cases is shown in Figure 5.1. Response amplitudes decreased for all modes in this frequency range, with the exception of the modes at 37 and 64 Hz. Response amplitude decreases were significant for the modes at 85 and 100 Hz, with the second mode in each case almost disappearing. Natural frequencies shifted lower for all modes with the exception of the modes at 48, 55 and 64 Hz. The frequency response of the test structure for the 100 to 200 Hz range for both the baseline and viscoelastic cases is shown in Figure 5.2. Significant decreases in frequency response amplitude were evident for all modes with the exception of the mode at 158 Hz. The mode at 147 Hz disappeared. Natural frequencies shifted lower for all modes with the exception of the mode at 158 Hz. The frequency response of the test structure for the 200 to 300 Hz range for both the baseline and viscoelastic cases is shown in Figure 5.3. All frequency response amplitudes for this frequency range were significantly lower than the baseline amplitudes. Four modes between 240 and 258 Hz disappeared completely. The entire frequency response curve shifted down and to the left in this frequency range. A mode appeared at 296 Hz that was previously at greater than 300 Hz and thus did not appear on the baseline plot.

Four narrow range frequency responses were obtained in order to increase the resolution at which response amplitude and percent damping measurements could be made. The frequency response of the test structure for the 25 to 45 Hz range for both the baseline and viscoelastic cases is shown in Figure 5.4. In this range, two out of three of the modes decreased in response amplitude, and all modes shifted lower in natural frequency. The natural frequency for the mode at 29.6 Hz dropped to 29.0 Hz, and its response amplitude dropped 4.6 dB. The natural frequency for the mode at 35.8 hz dropped to 35.6 Hz, and its response amplitude increased by 7.9 dB. The frequency response of the test structure for the 95 to 115 Hz range for both the baseline and viscoelastic cases is shown in Figure 5.5. Both modes in this range showed significant natural frequency shifts and amplitude response decreases. The natural frequency of the mode at 99.4 Hz shifted to 97.4 Hz, with the response amplitude decreasing by 16.0 dB. The natural frequency of the mode at 100.8 Hz shifted to 98.85 Hz, with the response amplitude decreasing by 12.6 dB. The frequency response of the test structure for the 120 to 140 Hz range for both the baseline and viscoelastic cases is shown in Figure 5.6. The double mode of the baseline structure shows up as one mode in the damped structure. The natural frequency for the mode at 126.3 Hz shifted to 123.8 Hz, with the response amplitude dropping by 12.4 dB. The natural frequency of the mode at 136.2 Hz shifted to 133.1 Hz, with the response amplitude dropping by 17.8 dB. The frequency response of the test structure for the 230 to 270 Hz range for both the baseline and viscoelastic cases is shown in Figure 5.7. The response amplitude of every mode in this range has been significantly reduced, with four of the six modes in this range disappearing after the application of the damping treatment. The natural frequency of the mode at 264 Hz decreased to 261.2 Hz, with the response amplitude decreasing by 14.5 dB.

The results for the measurements taken on the vane of the structure are generally the same as for those taken on the outer shell of the structure. As an example, the frequency response for the 15 to 115 Hz run is shown in Figure 5.8. As was the case in Figure 5.1, the higher frequency modes at 84 and 100 Hz showed large drops in response amplitude, while

the drops in response amplitude for the low frequency modes at 29 and 36 Hz were small. For the narrow frequency range run from 230 to 270 Hz shown in Figure 5.9, the vane measurement was similar to the outer shell measurement shown in Figure 5.7. All modes either disappeared or had their response amplitudes greatly reduced. Even the mode at 243 Hz, which shows up strongly in the vane measurement, was reduced in amplitude by 19 dB.

## 2. Case with Viscoelastic Material on Outer Shell and Vanes

The frequency responses for the case with viscoelastic material on the outer shell and on the vane are shown in Figures 5.10 through 5.18. The curves were different from those taken with viscoelastic material on the outer shell only since modal response amplitude reductions and increases were magnified slightly by the addition of the viscoelastic material on the vanes. For instance, the response amplitude of the mode at 100 Hz, as seen in Figure 5.14, decreased by 17.5 dB versus 16 dB for the case with viscoelastic material only on the outer shell. Also, the response amplitude for the mode at 264 Hz, as shown in Figure 5.16, decreased by 16.5 dB versus 14.5 dB for the case with viscoelastic material only on the outer shell. Interestingly, the 36 Hz mode that experienced a sizable increase in response amplitude due to the application of the damping treatment on the outer shell had its response amplitude increased even more for the case of viscoelastic material on both outer shell and vane. The response amplitude for this case, as seen in Figure 5.13, increased 12.5 dB versus 7.9 dB for the case with viscoelastic material on the outer shell only.

Measurements taken on the vane for this case were similar to the measurements taken on the outer shell. Response amplitudes generally decreased similar amounts and frequency shifts were also similar.

## B. COMPARISON WITH MODAL STRAIN ENERGY METHOD

The frequency response results for the Modal Strain Energy(MSE) Method versus the case of viscoelastic material on the outer shell only are found in Figures 5.19 through 5.25. The correlation between the frequency

response predicted by the MSE method and the results obtained experimentally was not good. Natural frequencies predicted by the MSE method were lower than those obtained experimentally for frequencies less than the mid range (150 Hz) frequency, and natural frequencies predicted by the MSE method were higher than those obtained experimentally for higher than mid range frequencies. The MSE curves generally showed amplitudes higher than those found by experimentation, and generally showed less damping. Also, occasional modes appear in the MSE curves that did not show up in testing. Note that the experimental curve in Figure 5.23 actually has its mode at 97 Hz, and is thus approximately 10 Hz higher than the MSE prediction.

#### C. STRUCTURAL DAMPING

Structural damping was measured for four modes for each damping treatment case using the half power bandwidth method. Structural damping as a percentage of critical damping is shown in Figure 5.26. All cases are for measurements taken on the outer shell. As shown in Figure 5.26, the undamped test structure is an extremely lightly damped structure. Addition of the constrained layer viscoelastic damping treatment to the outer shell increased percent damping by 1.5 to 8 times. Further addition of the damping material to the vane resulted in marginally higher damping in three out of four cases. The highest damping recorded was 1.044 percent for the mode at 123.7 Hz with damping material applied to the outer shell and vane. Many modes, especially in the 230 to 270 Hz range, could not be plotted since addition of damping treatments made the modes completely disappear or made them rise less than the 3 dB required to get a damping measurement using the half power bandwidth method. The MSE method underpredicted the amount of damping obtained.

#### D. DISCUSSIONS

The addition of a constrained layer viscoelastic damping treatment was seen to be a very effective method of controlling large resonant vibrations in the test structure. Most modes had response amplitude

reductions in the 15 dB area, with some modes disappearing completely. This was accomplished with a damping treatment which weighed 12.9 pounds, or approximately two percent of the total weight of the approximately 650 pound structure. Also, structural integrity of the test structure was not adversely affected by the addition of the damping treatment.

Addition of the damping treatment to the vane as well as the outer shell was found to be only marginally more effective in controlling resonant vibrations. Response amplitude reductions were only slightly larger with the addition of the damping treatment to the vane. This was expected due to the large percent of test structure motion that occurred in the outer shell area, as determined by the mode shape and strain energy analyses. In summary, if most of the motion occurs in the outer shell, most of the energy dissipation will occur there also.

Vibration energy dissipation was worst in the low frequency region below 75 Hz. This was due to the low shear modulus of 3M ISD-112 in this area. As equation 2.11 shows, the energy dissipation in a constrained layer system is directly dependent on the shear modulus. As Figure 3.13 shows, the shear modulus of 3M ISD-112 in the area from 20 to 75 Hz is only 50 to 100 PSI. This is simply too low to provide good energy dissipation. In effect, the viscoelastic material just "gives", causing great reductions in possible energy dissipation.

The response amplitude for the second mode at 36 Hz actually increased with the addition of the constrained layer damping treatment. As seen in Figure 3.3, the outer shell did move in this mode but experienced almost no deformation, while the vane experienced a large bending deformation. Thus, application of a damping treatment to the outer shell provided no energy dissipation at all, and the added mass of the damping treatment caused the vane to experience a larger deformation. This caused the response amplitude to increase. Likewise, addition of the damping treatment to the vane only increased the mass more, causing any energy dissipation which may have occurred in the vane to be overshadowed by the increases in response amplitude. Also possibly contributing was the presence of entrapped air in both the outer shell and vane damping

treatments. These air pockets contributed to a reduction in damping treatment effectiveness [Refs. 2,14]. Although difficult to quantify, the presence of imperfections in the viscoelastic bond to the test structure could have contributed to the increases in response amplitude seen in the second mode. Of course, energy dissipation at all modes would probably improve if the air pockets could be completely removed.

The MSE method did not give a good prediction of the experimental results obtained. In general, the MSE method tended to show response amplitudes that were too high with too little damping. In addition, some extra modes appeared in the MSE method results that did not appear during experimentation. The reasons for these results are as follows:

- The bolts which connect the inner and outer shells to the vanes of the test structure were not modeled in the finite element analysis. The finite element analysis assumed that the test structure was a smooth, continuous structure. Actually, the structure contained 144 bolts, with 96 bolts contained in the inner shell, and 48 bolts contained in the outer shell. These bolts acted as stiff clamps, holding the vanes and outer shell in place, thereby reducing the response amplitudes of those sections of the test structure. Since the finite element model did not model these bolts, the MSE method predicted higher responses than were obtained.
- The aspect ratio is the ratio of the length of the longest to the shortest side for a finite element. An aspect ratio of one is the most desirable case since high aspect ratio elements cause large errors to be introduced into a finite element analysis. The aspect ratio for the CHEXA elements used to model the viscoelastic material of the test structure was 294.7. Although Kienholz and Johnson have reported adequate results for simple structures with aspect ratios this high [Ref. 1], the high aspect ratio warning message issued by MSC/NASTRAN during the analysis indicates that this was a source of error.
- When modeling a curved structure using flat elements, the included angle of the flat elements should be 10 degrees or less to obtain

displacement errors of four percent or less [Ref. 15]. In fact, even smaller included angles may be required when performing modal analysis as was performed for this analysis [Ref. 15]. The included angle for the outer shell elements of the finite element model was 22.5 degrees, and the included angle for the inner shell elements was 45 degrees. This coarseness in the finite element model undoubtedly contributed to the less than exact results obtained with the MSE method.

- The viscoelastic material properties used in the finite element model were found from Figure 3.8, which was provided by 3M Corporation. However, the material property curves used by Maurer [Ref. 2], found in Vibration Damping [Ref. 4] and used by Drake [Ref. 13] in designing damping treatments with 3M ISD - 112 are all different. In addition, Drake and Kluesener [Ref. 16] showed that different material property curves were obtained depending on how the properties were measured. In summary, there is no consensus on exactly what the material properties of 3M ISD-112 are, and thus it is possible that the material property values used in the finite element model were inaccurate. This possibility is reinforced by the fact that the shear modulus found from Figure 3.8 was low compared to the value found from the other sources stated above, and the damping predicted by the MSE method turned out to be low also.
- Viscoelastic material property values of different samples of the same material tend to vary slightly. Thus, even if the finite element model used material property values that were accurate as average values, it is possible that the actual viscoelastic material used during experimentation had material property values that differed from the values used in the prediction.

The results obtained by the MSE method were conservative. Response amplitudes were generally higher than those obtained by testing, and damping was less than testing showed.

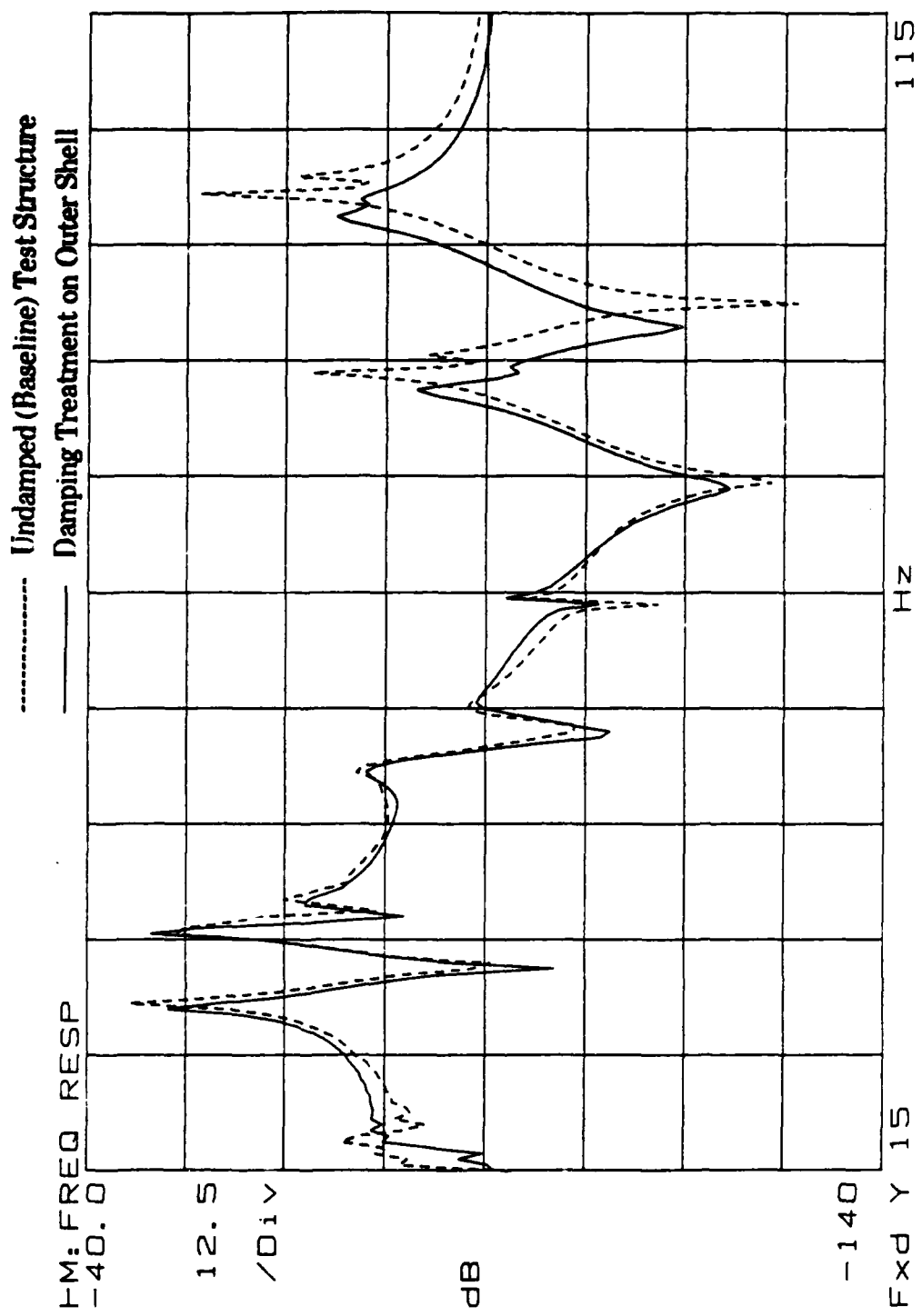


Figure 5.1. Frequency response measured on outer shell of test structure, damping treatment applied to outer shell area, 15 to 115 Hz.

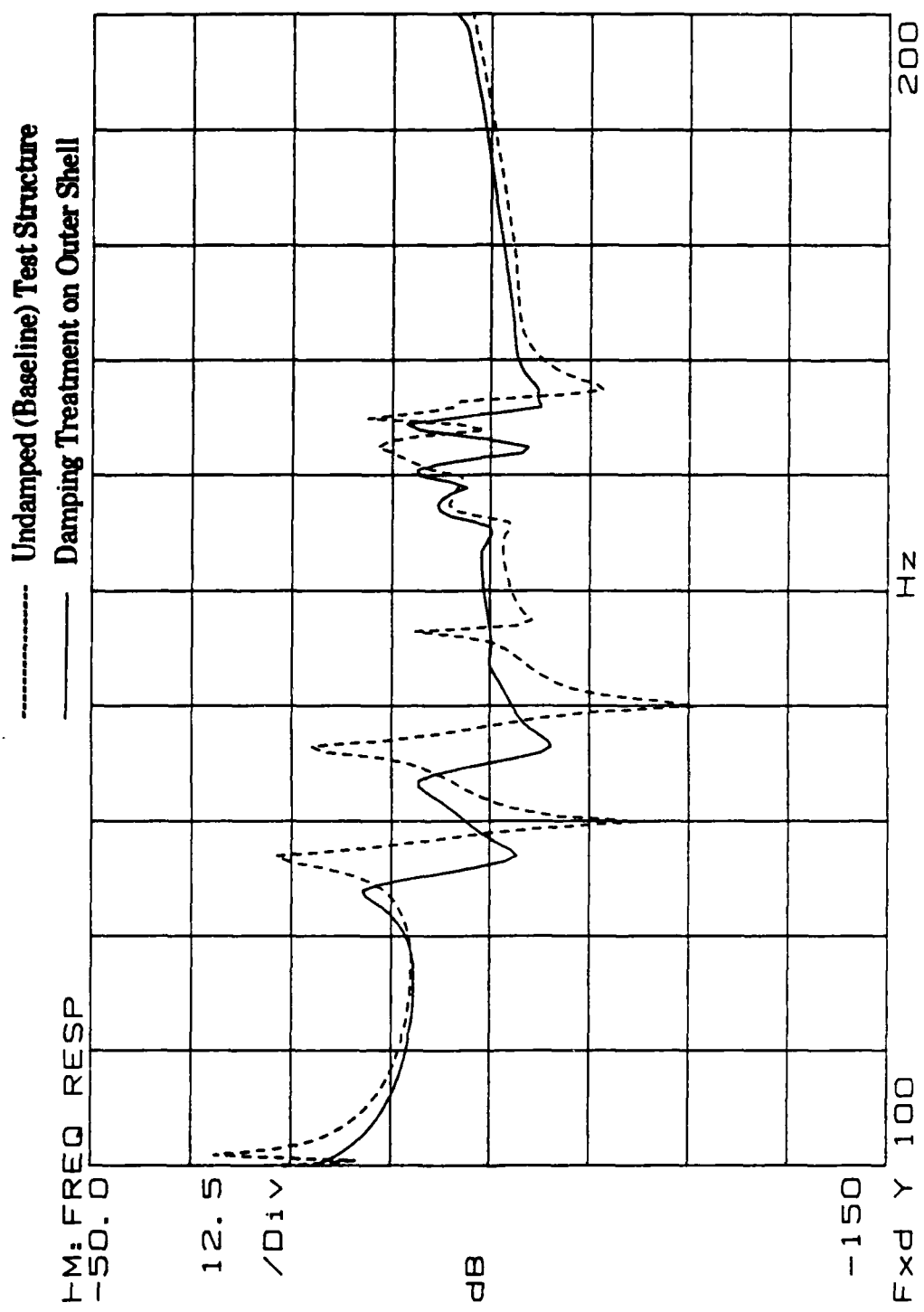


Figure 5.2. Frequency response measured on outer shell of test structure, damping treatment applied to outer shell area, 100 to 200 Hz.

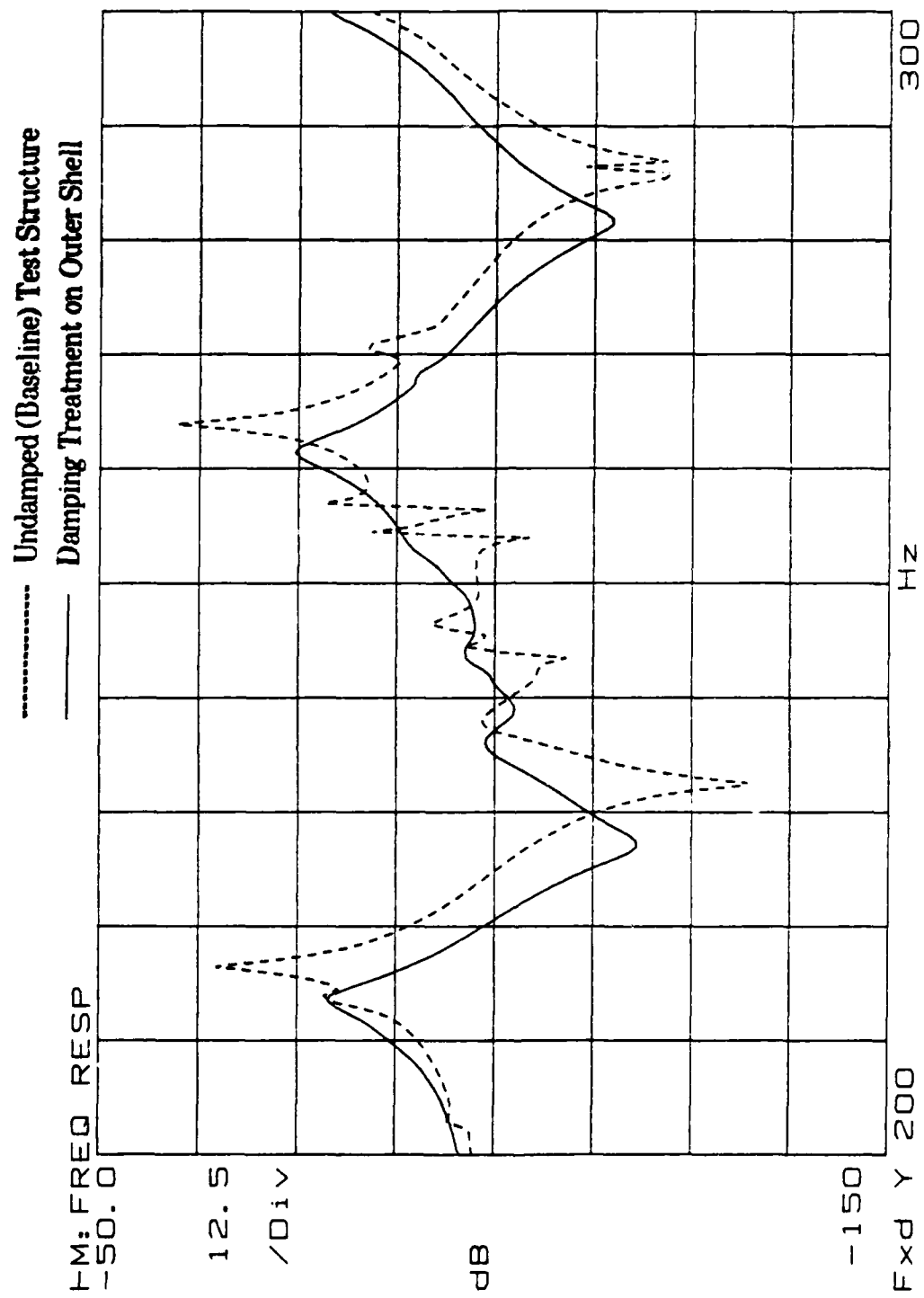


Figure 5.3. Frequency response measured on outer shell of test structure, damping treatment applied to outer shell area, 200 to 300 Hz.

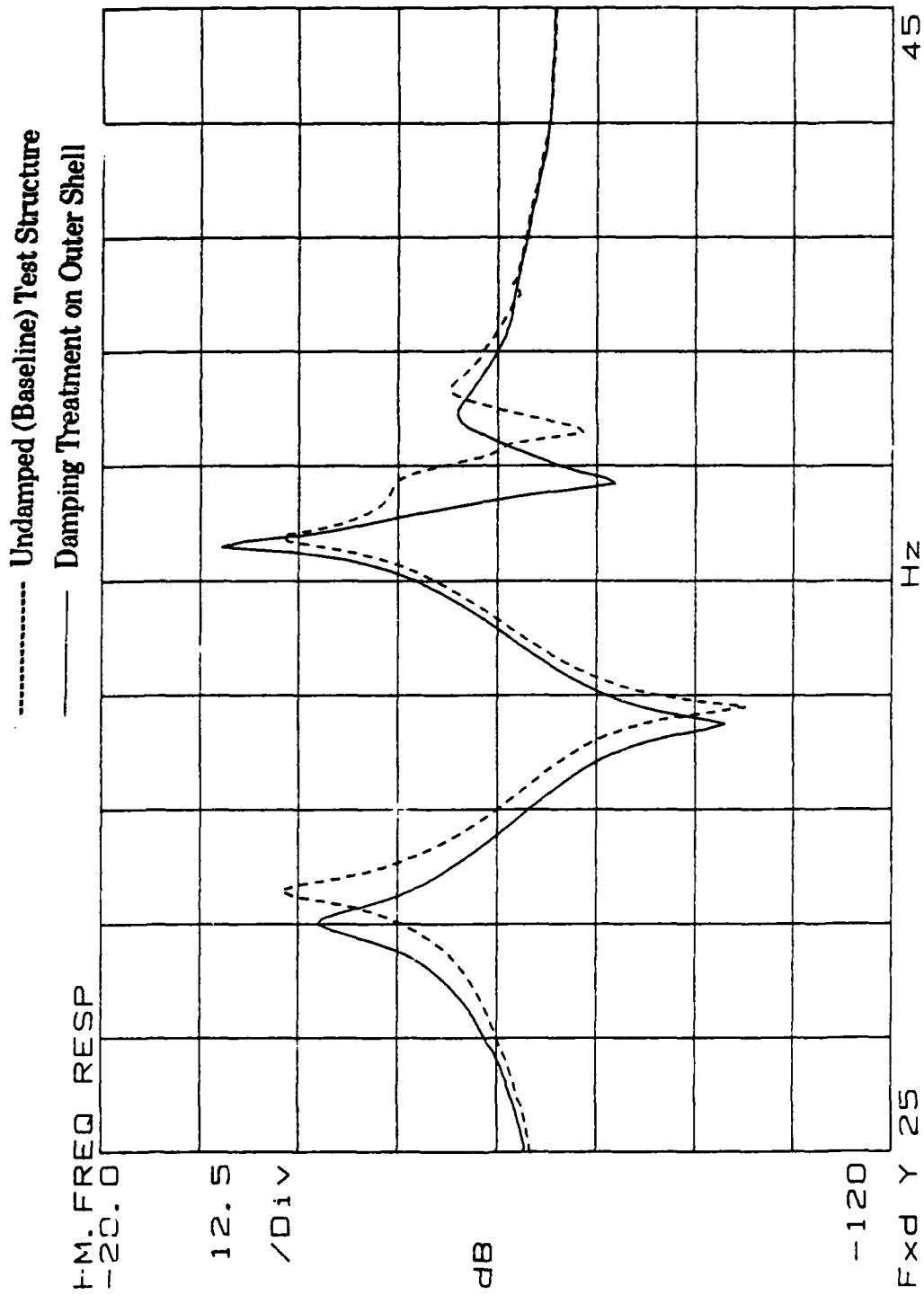


Figure 5.4. Frequency response measured on outer shell of test structure, damping treatment applied to outer shell area, 25 to 45 Hz.

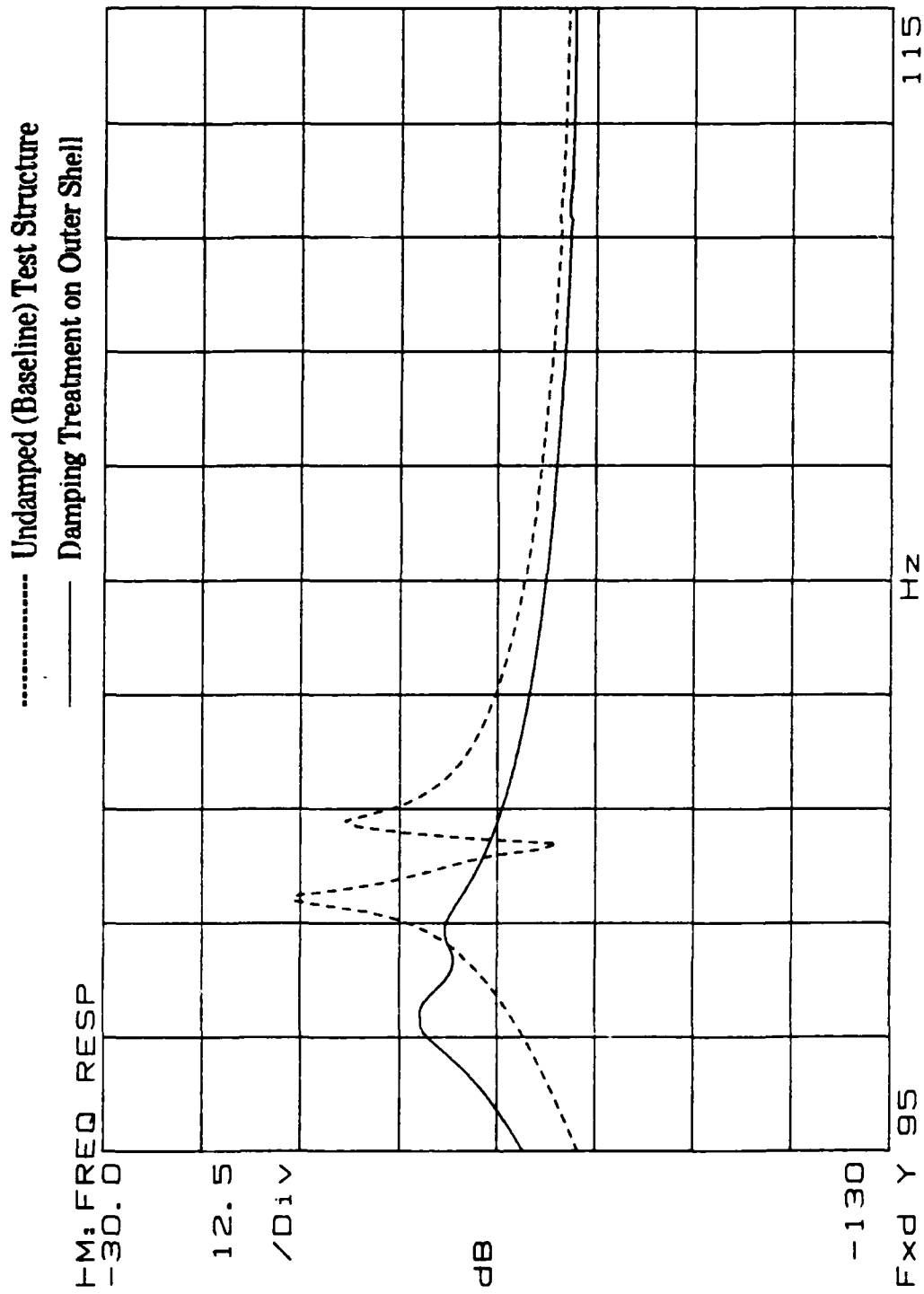


Figure 5.5. Frequency response measured on outer shell of test structure, damping treatment applied to outer shell area, 95 to 115 Hz.

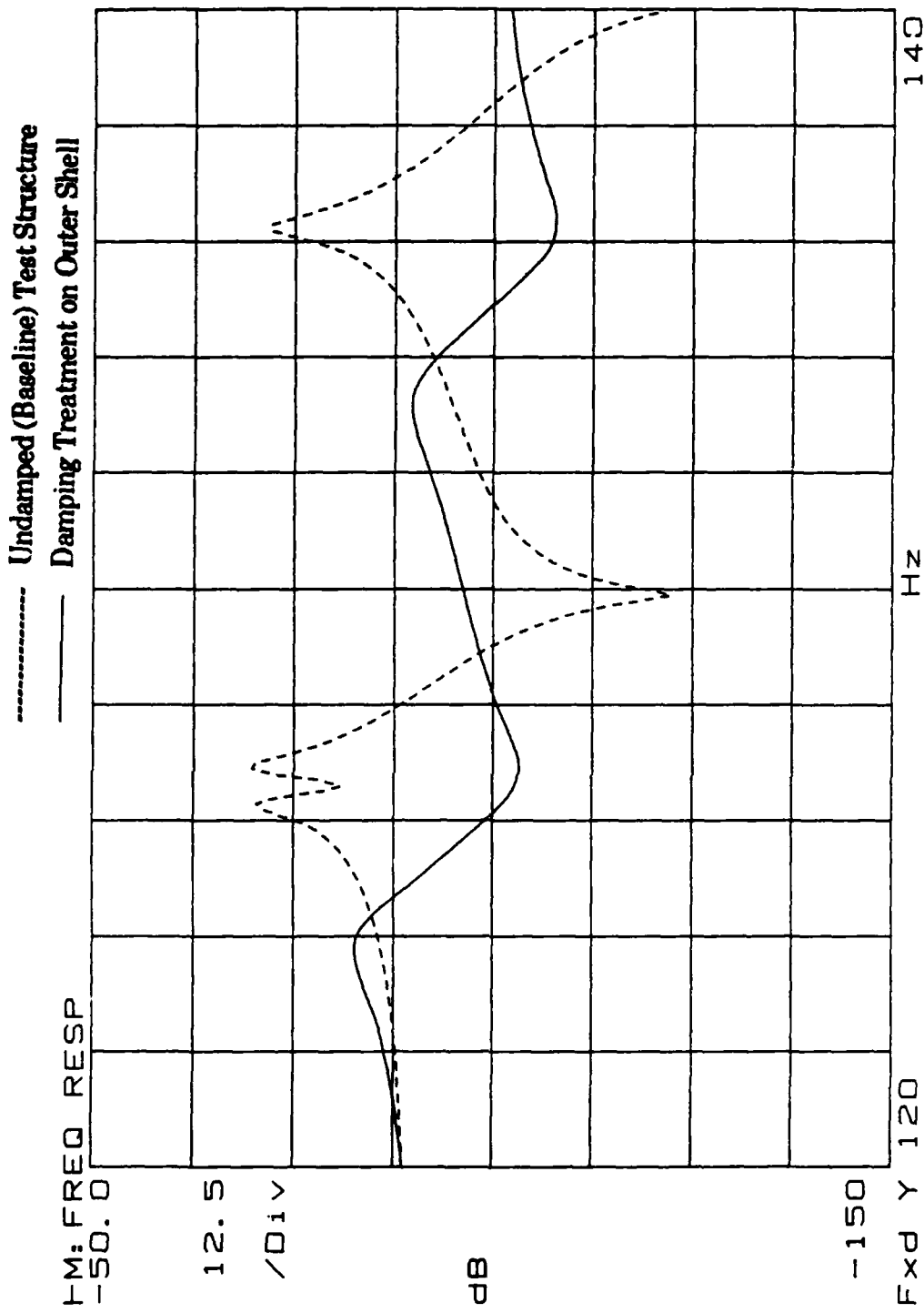


Figure 5.6. Frequency response measured on outer shell of test structure, damping treatment applied to outer shell area, 120 to 140 Hz.

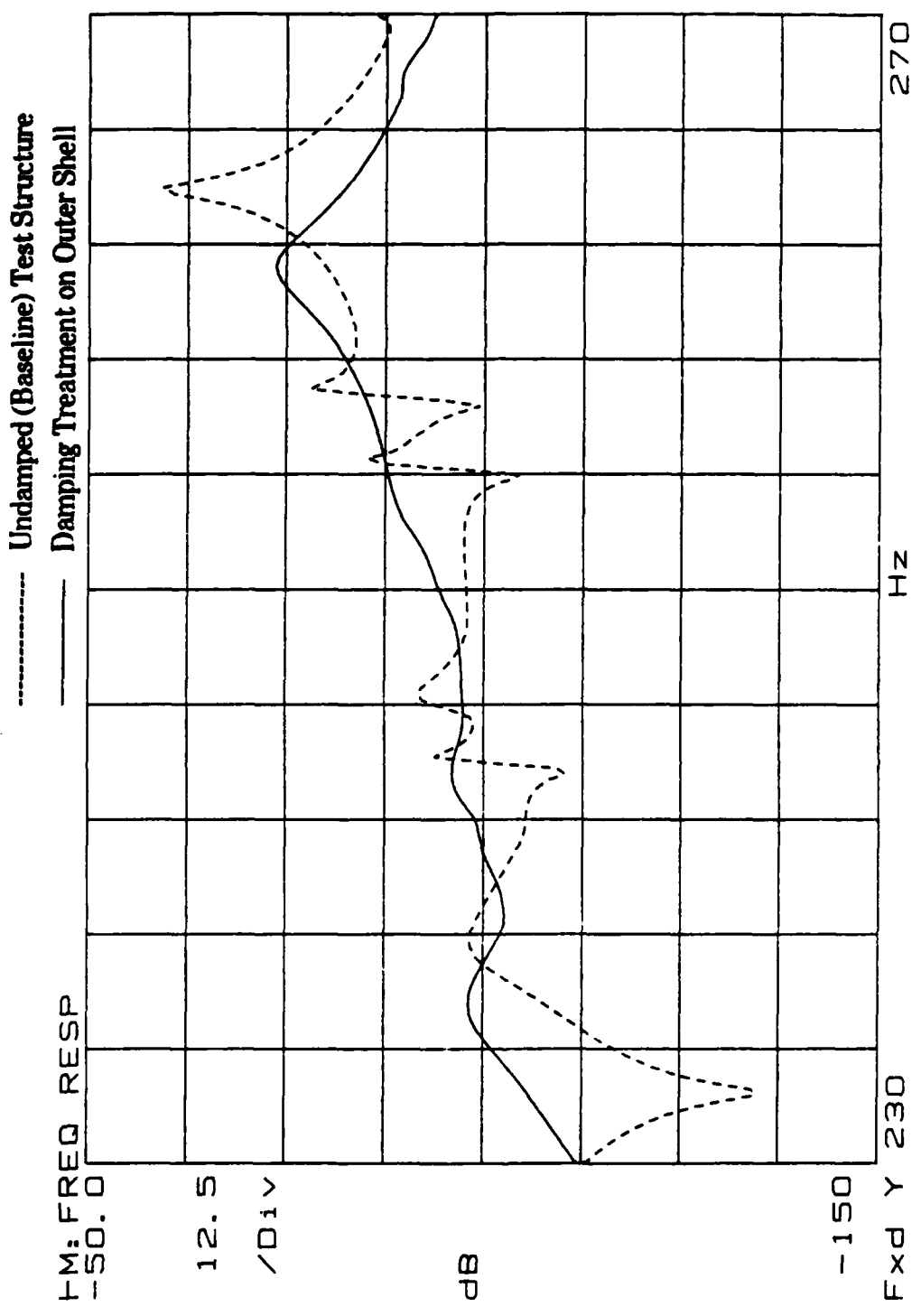


Figure 5.7. Frequency response measured on outer shell of test structure, damping treatment applied to outer shell area, 230 to 270 Hz.

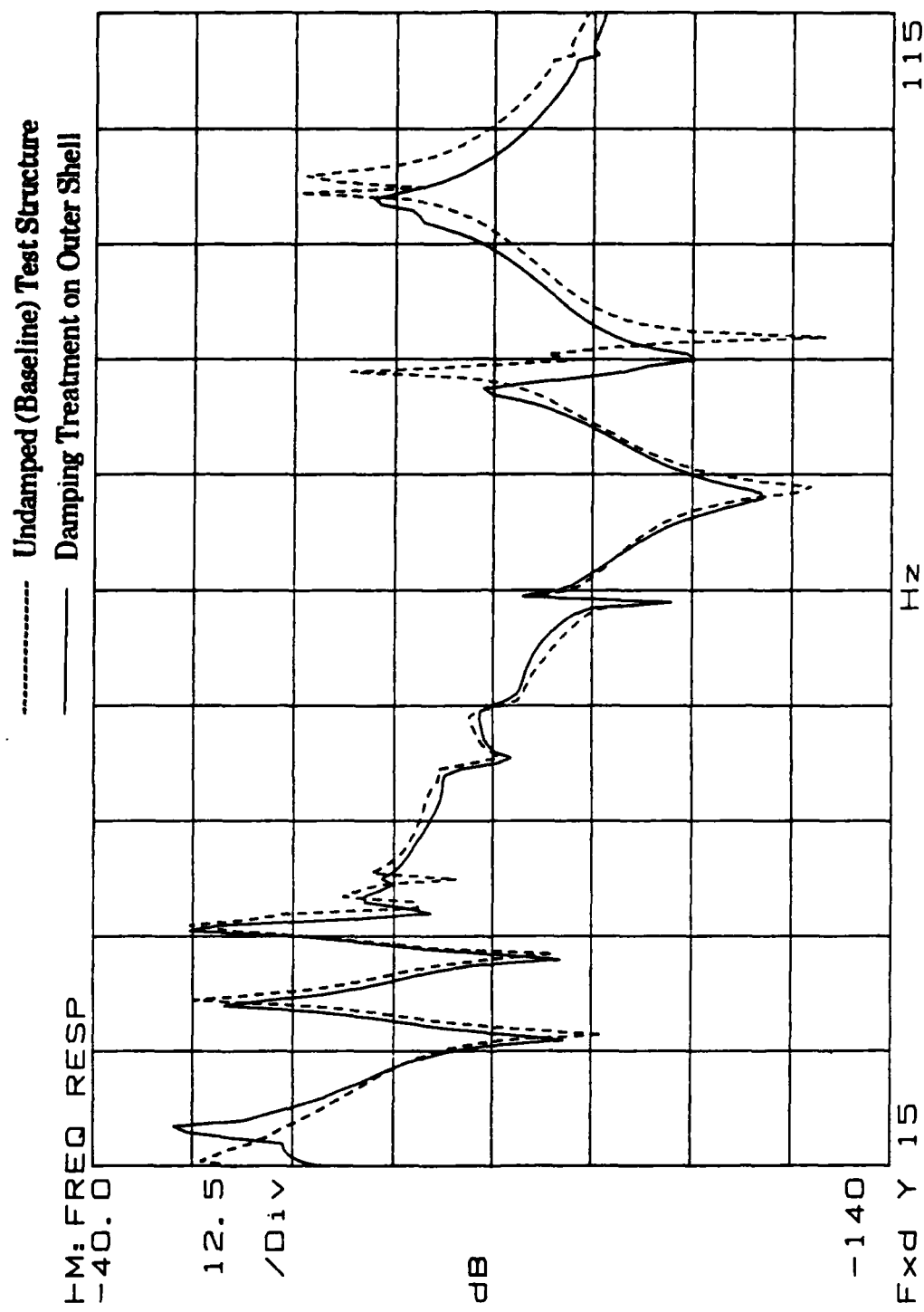


Figure 5.8. Frequency response measured on vane of test structure, damping treatment applied to outer shell area, 15 to 115 Hz.

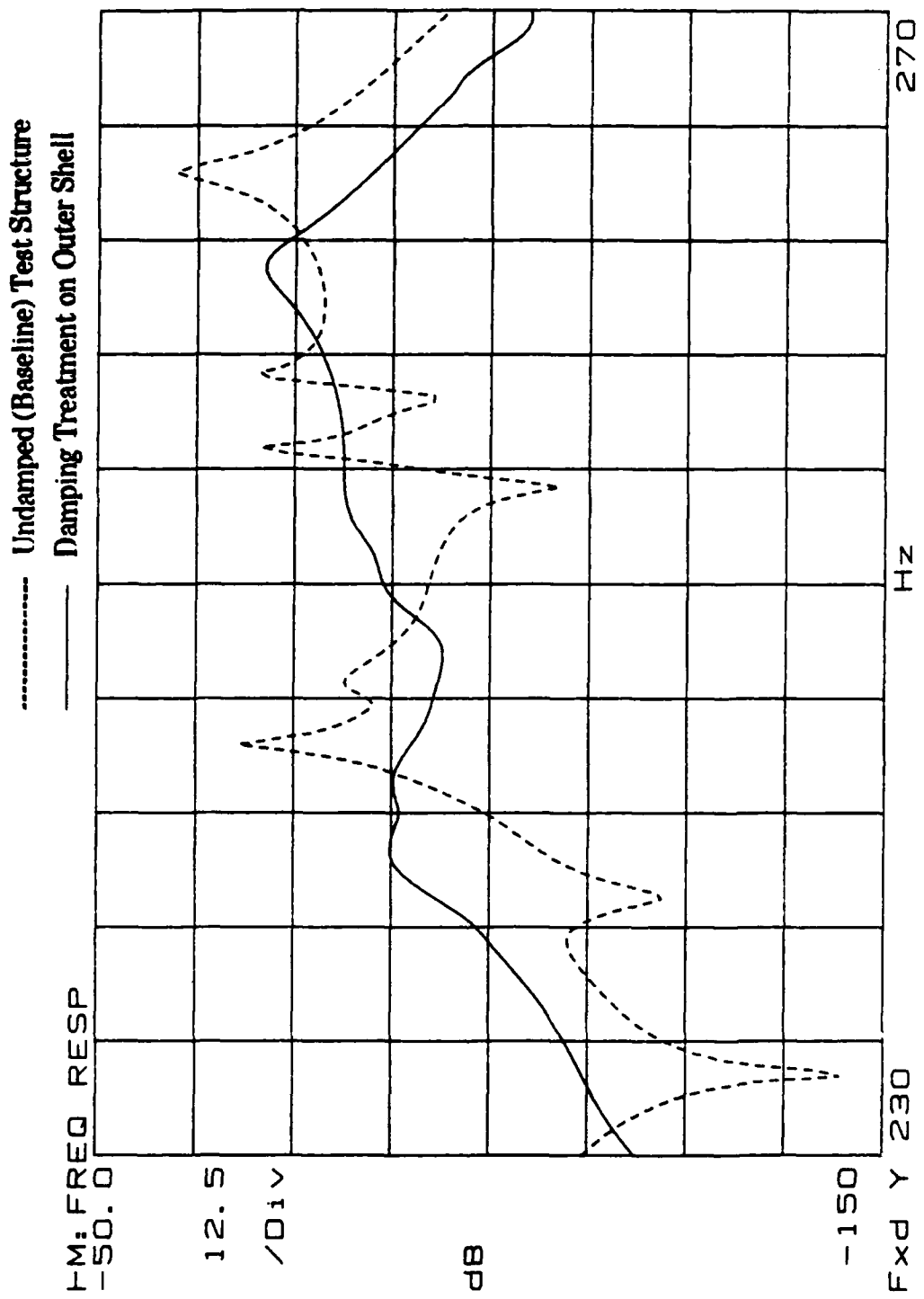


Figure 5.9. Frequency response measured on vane of test structure,  
damping treatment applied to outer shell area, 230 to 270 Hz .

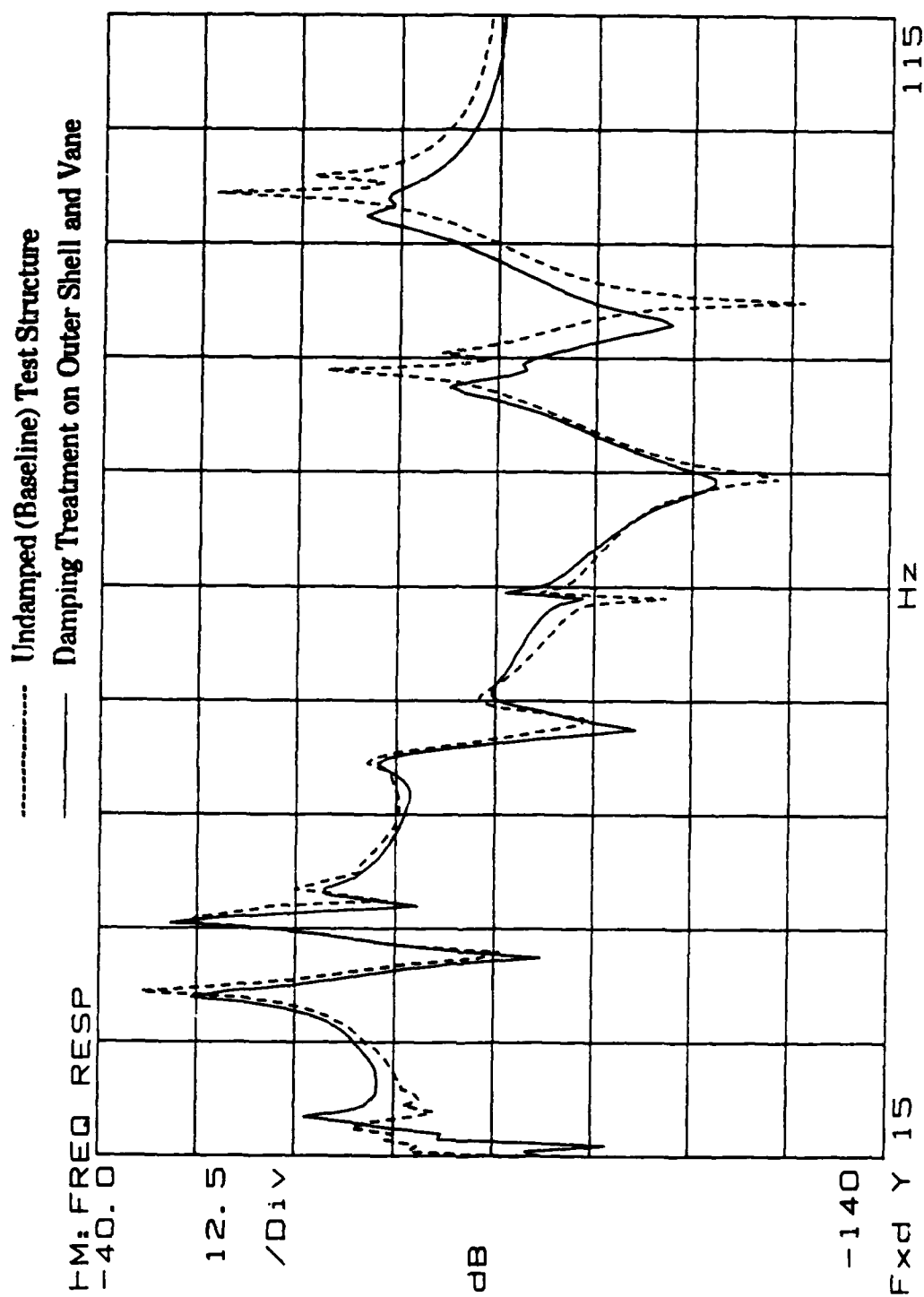


Figure 5.10. Frequency response measured on outer shell of test structure, damping treatment applied to outer shell and vane areas, 15 to 115 Hz .

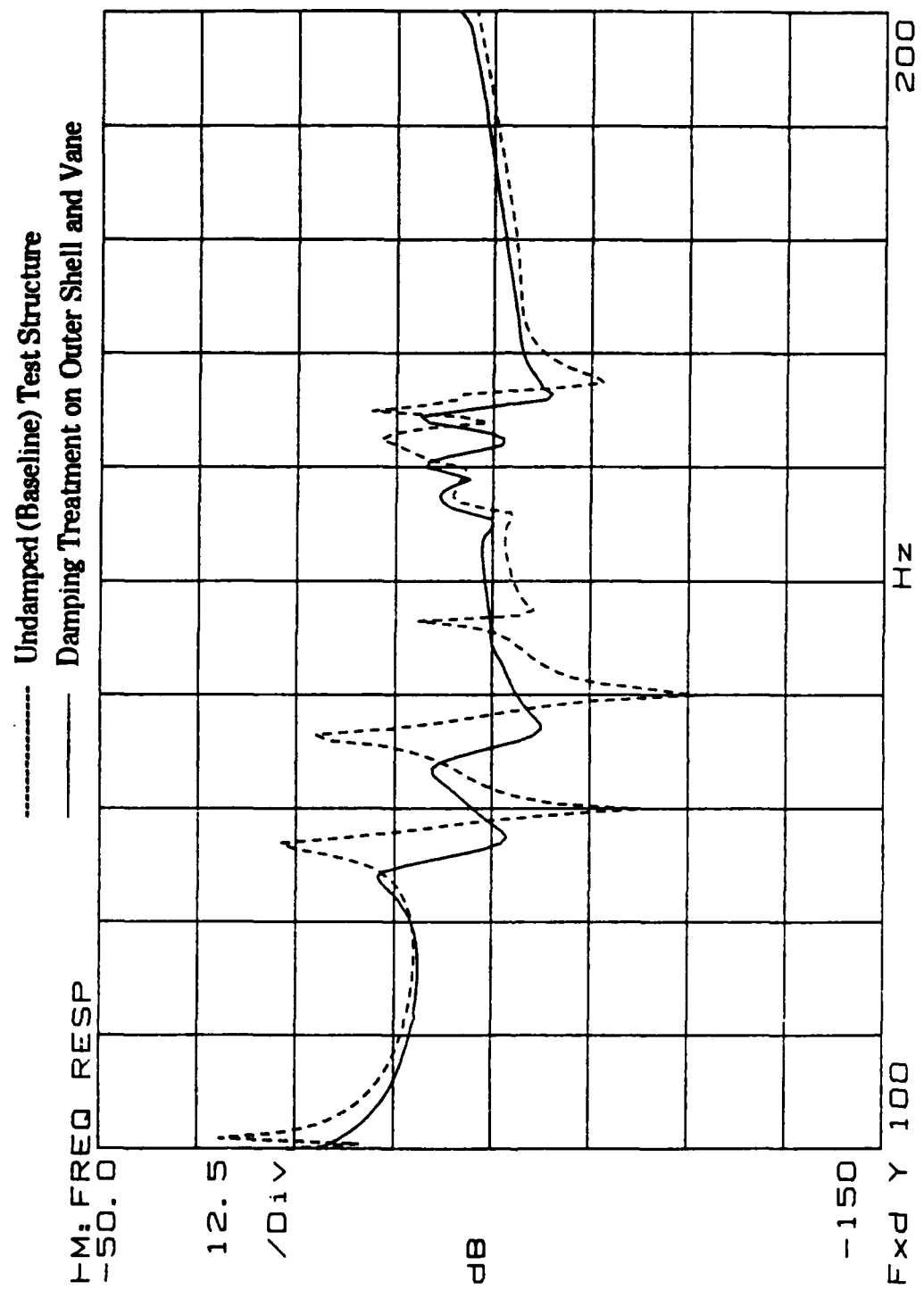


Figure 5.11. Frequency response measured on outer shell of test structure, damping treatment applied to outer shell and vane areas, 100 to 200 Hz .

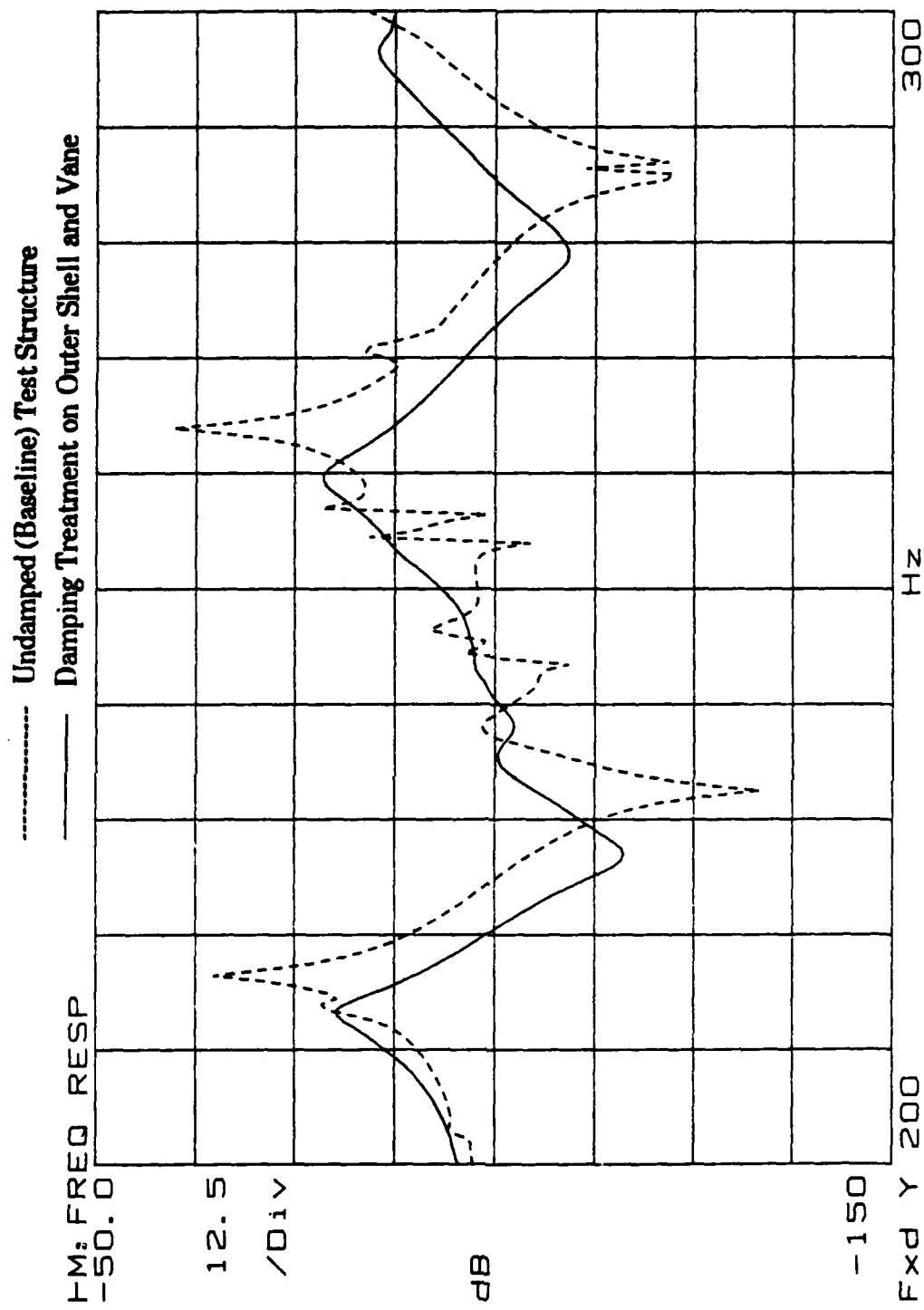


Figure 5.12. Frequency response measured on outer shell of test structure, damping treatment applied to outer shell and vane areas, 200 to 300 Hz .

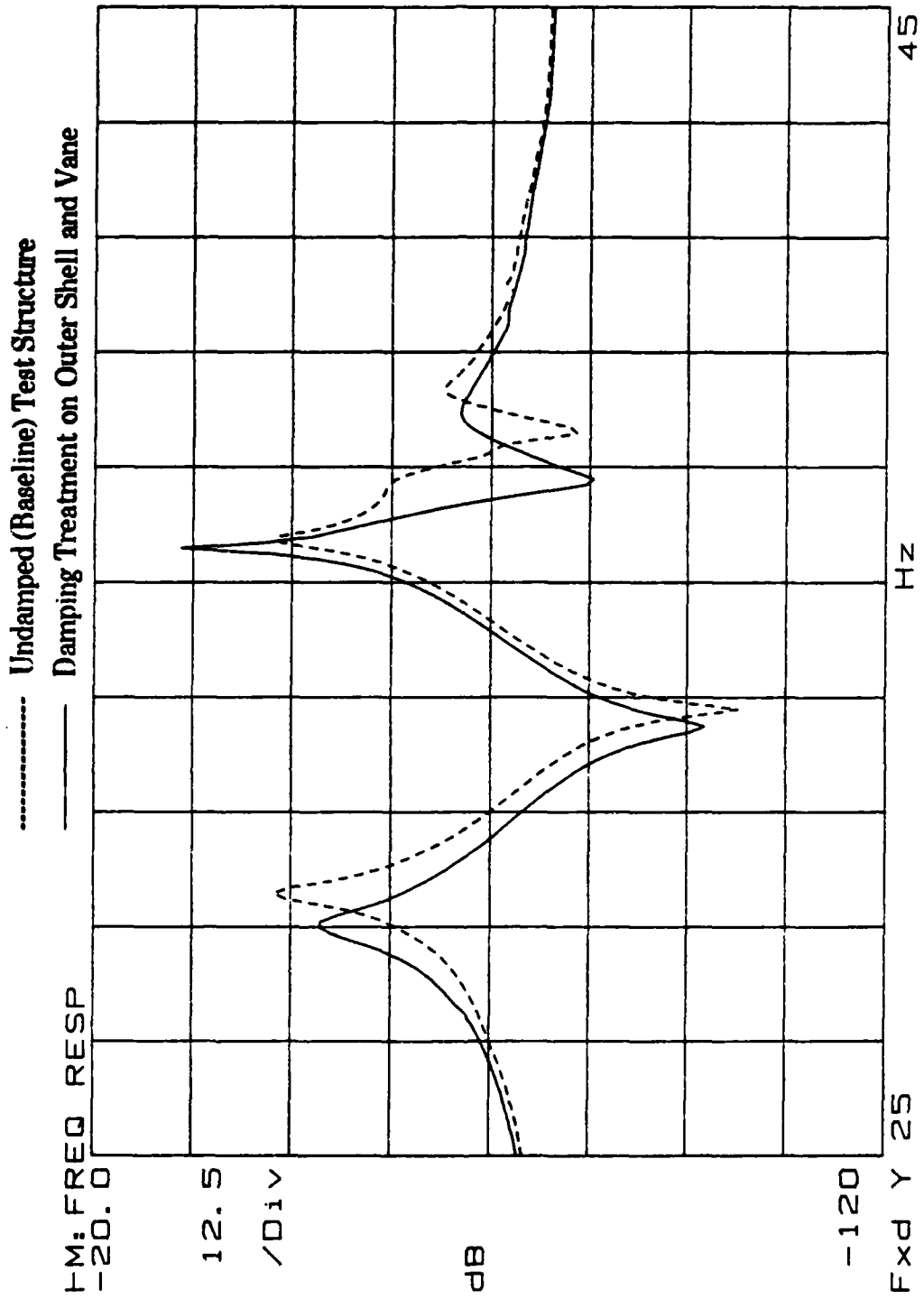


Figure 5.13. Frequency response measured on outer shell of test structure,  
damping treatment applied to outer shell and vane areas, 25 to 45 Hz .

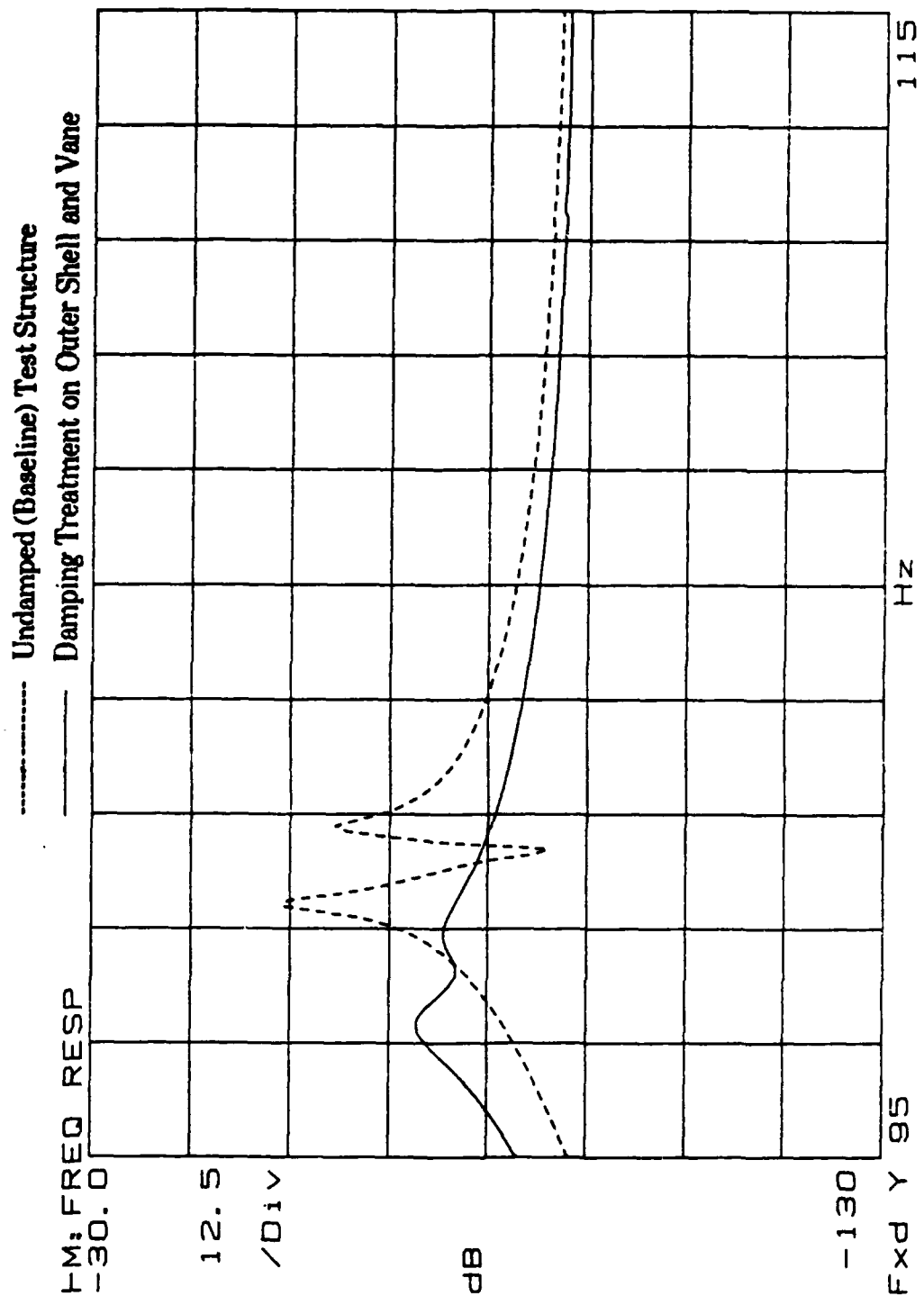


Figure 5.14. Frequency response measured on outer shell of test structure, damping treatment applied to outer shell and vane areas, 95 to 115 Hz .

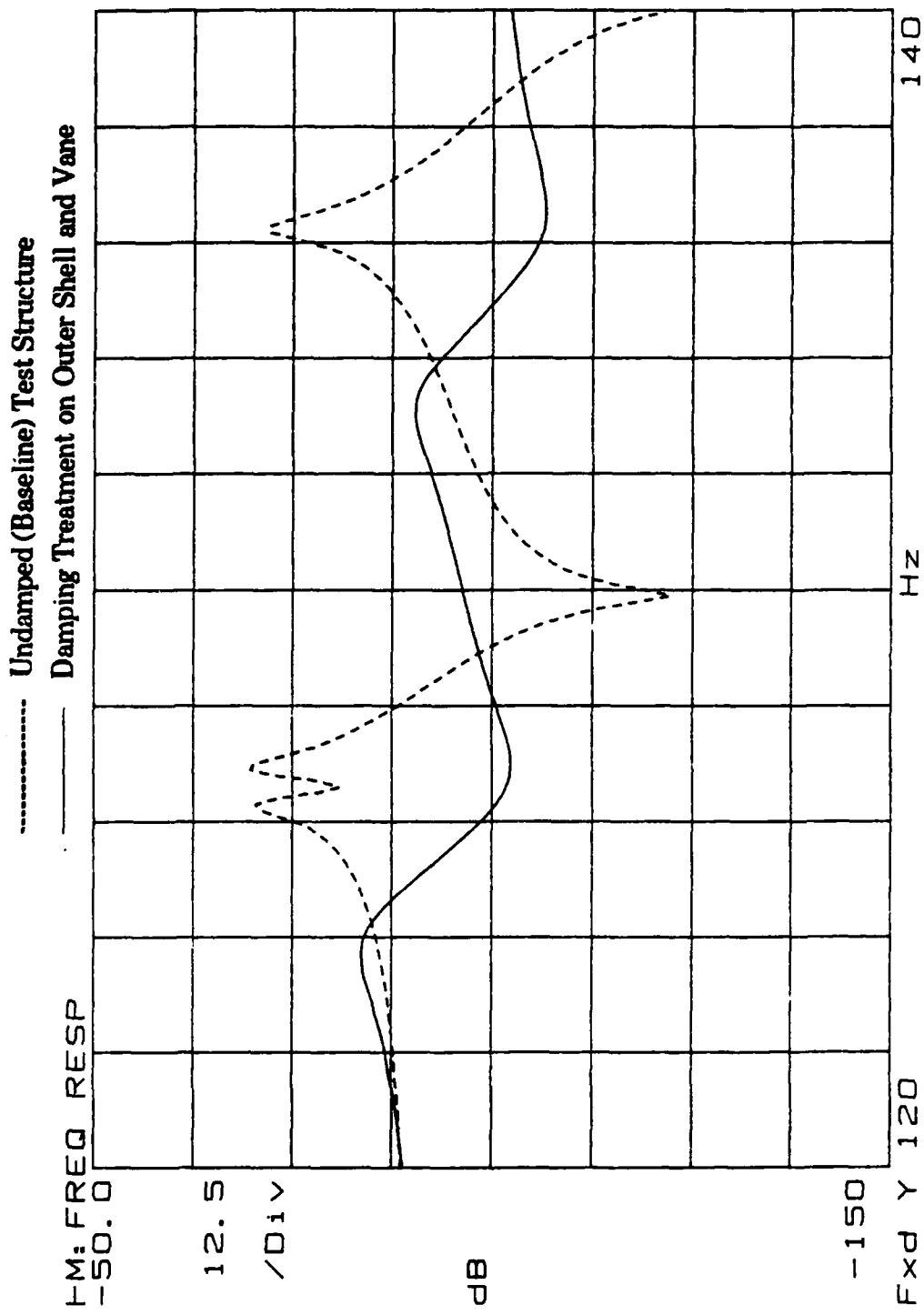


Figure 5.15. Frequency response measured on outer shell of test structure, damping treatment applied to outer shell and vane areas, 120 to 140 Hz .

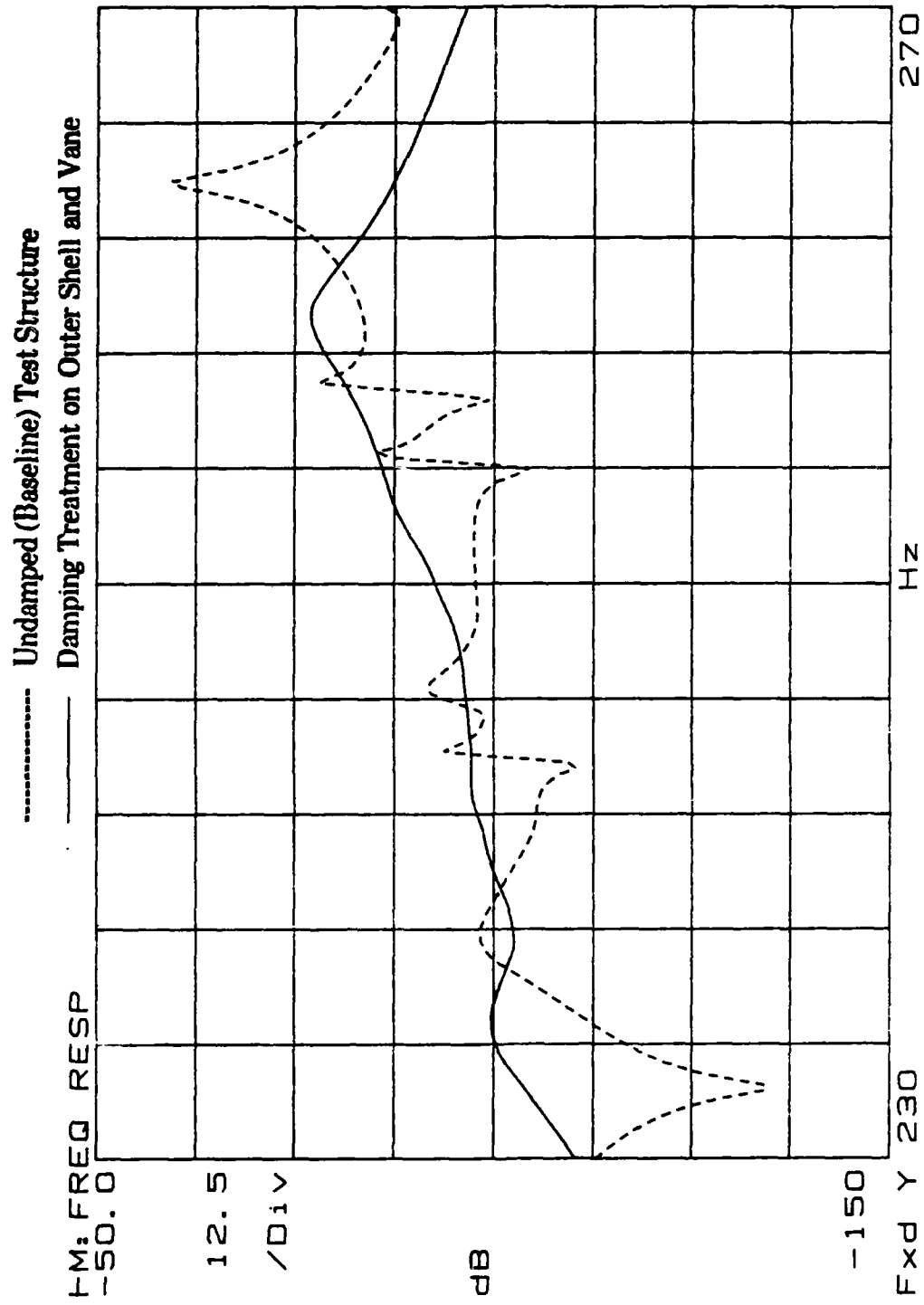


Figure 5.16. Frequency response measured on outer shell of test structure, damping treatment applied to outer shell and vane areas, 230 to 270 Hz .

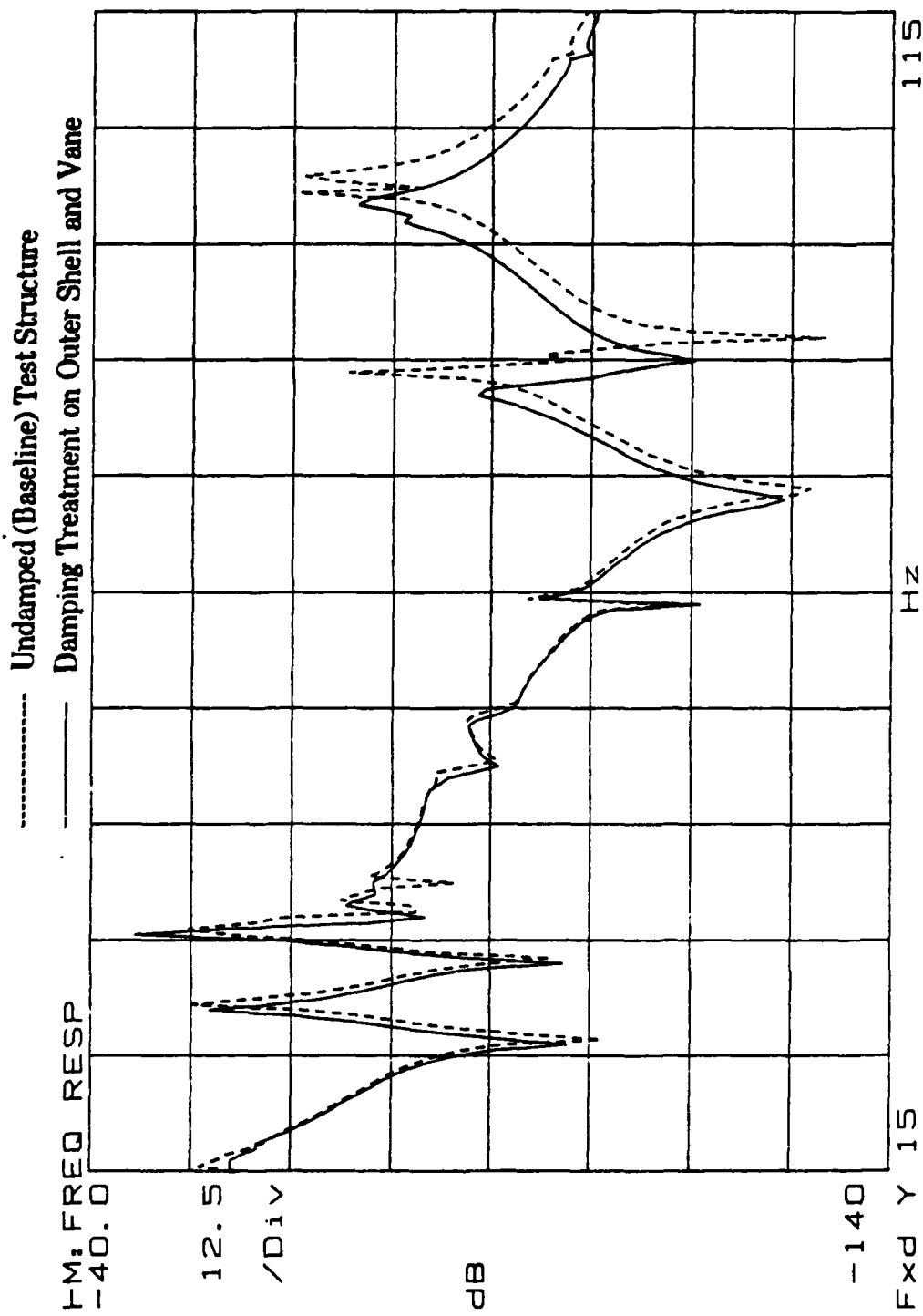


Figure 5.17. Frequency response measured on vane of test structure, damping treatment applied to outer shell and vane areas, 15 to 115 Hz .

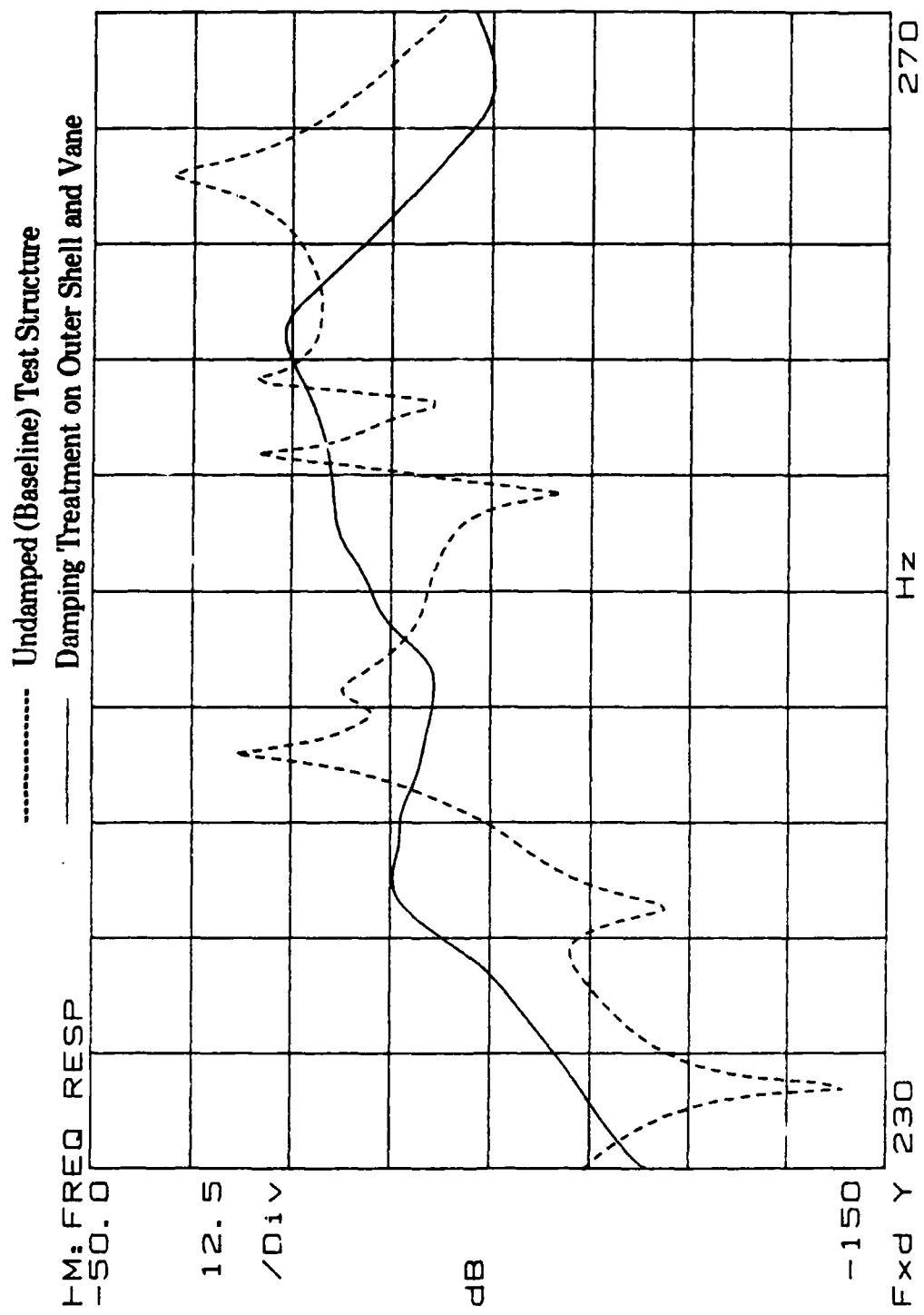


Figure 5.18. Frequency response measured on vane of test structure, damping treatment applied to outer shell and vane areas, 230 to 270 Hz .

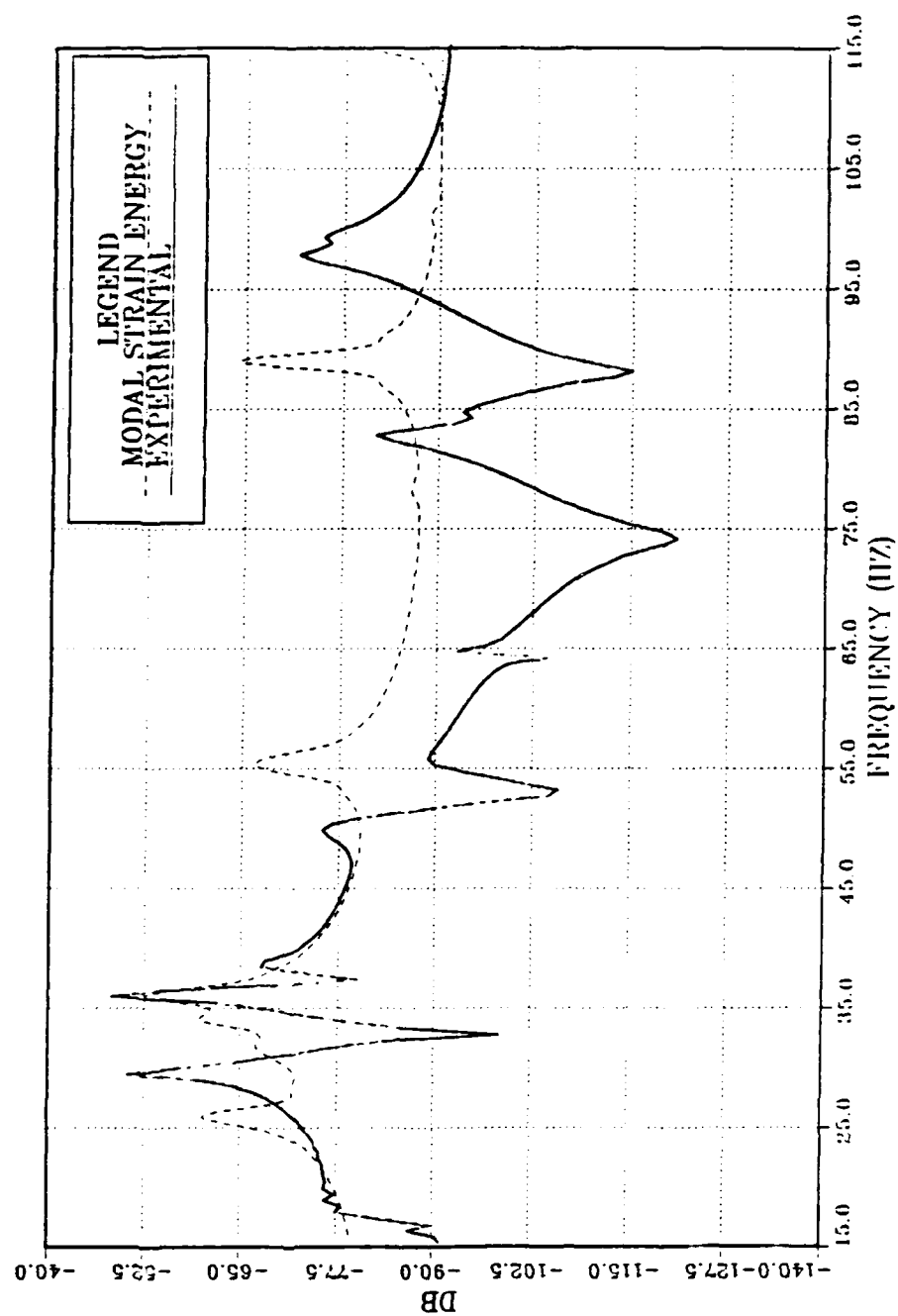


Figure 5.19. Modal Strain Energy method vs experimental frequency response, damping treatment applied to outer shell area, 15 to 115 Hz .

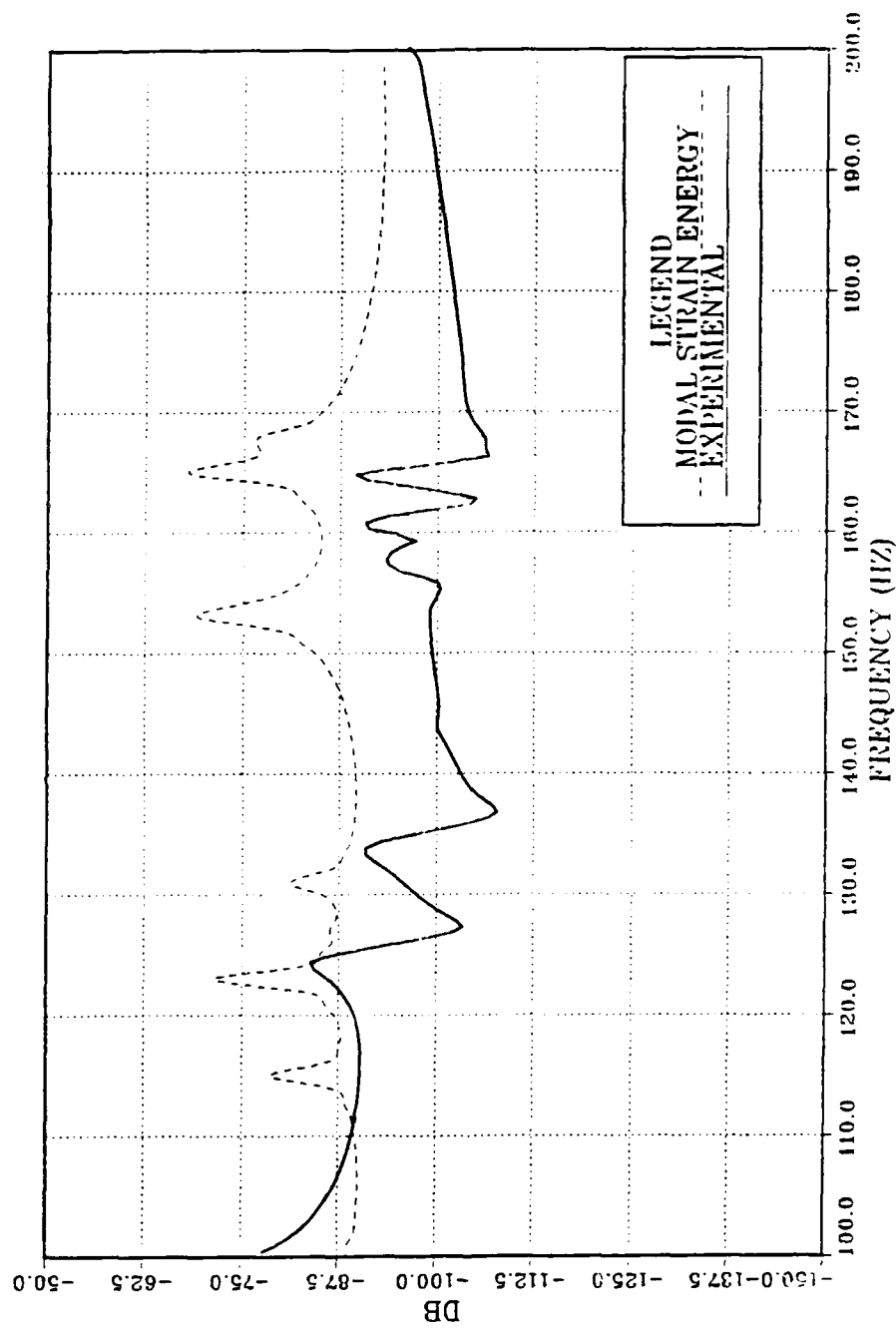


Figure 5.20. Modal Strain Energy method vs experimental frequency response, damping treatment applied to outer shell area, 100 to 200 Hz .

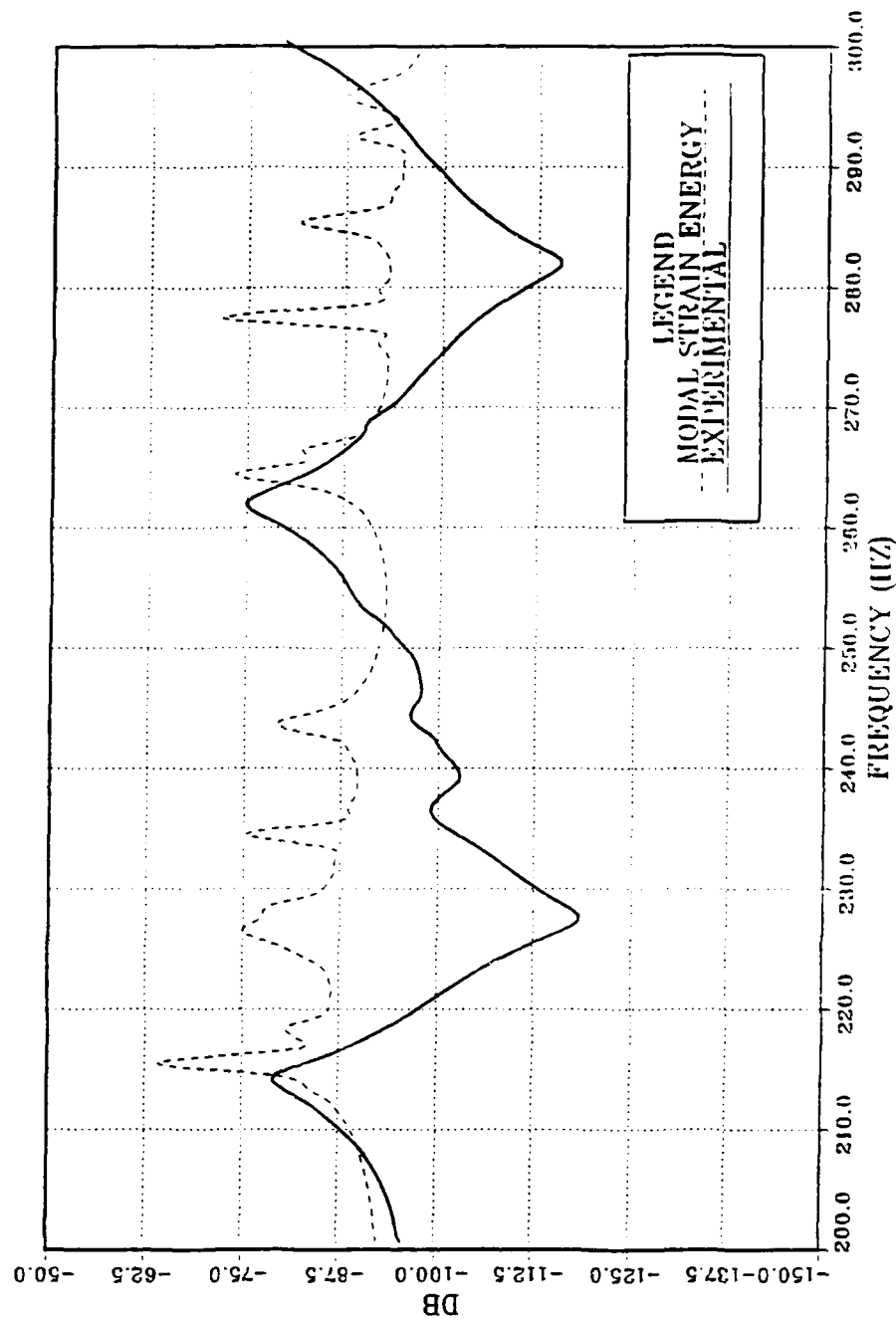


Figure 5.21. Modal Strain Energy method vs experimental frequency response, damping treatment applied to outer shell area, 200 to 300 Hz .

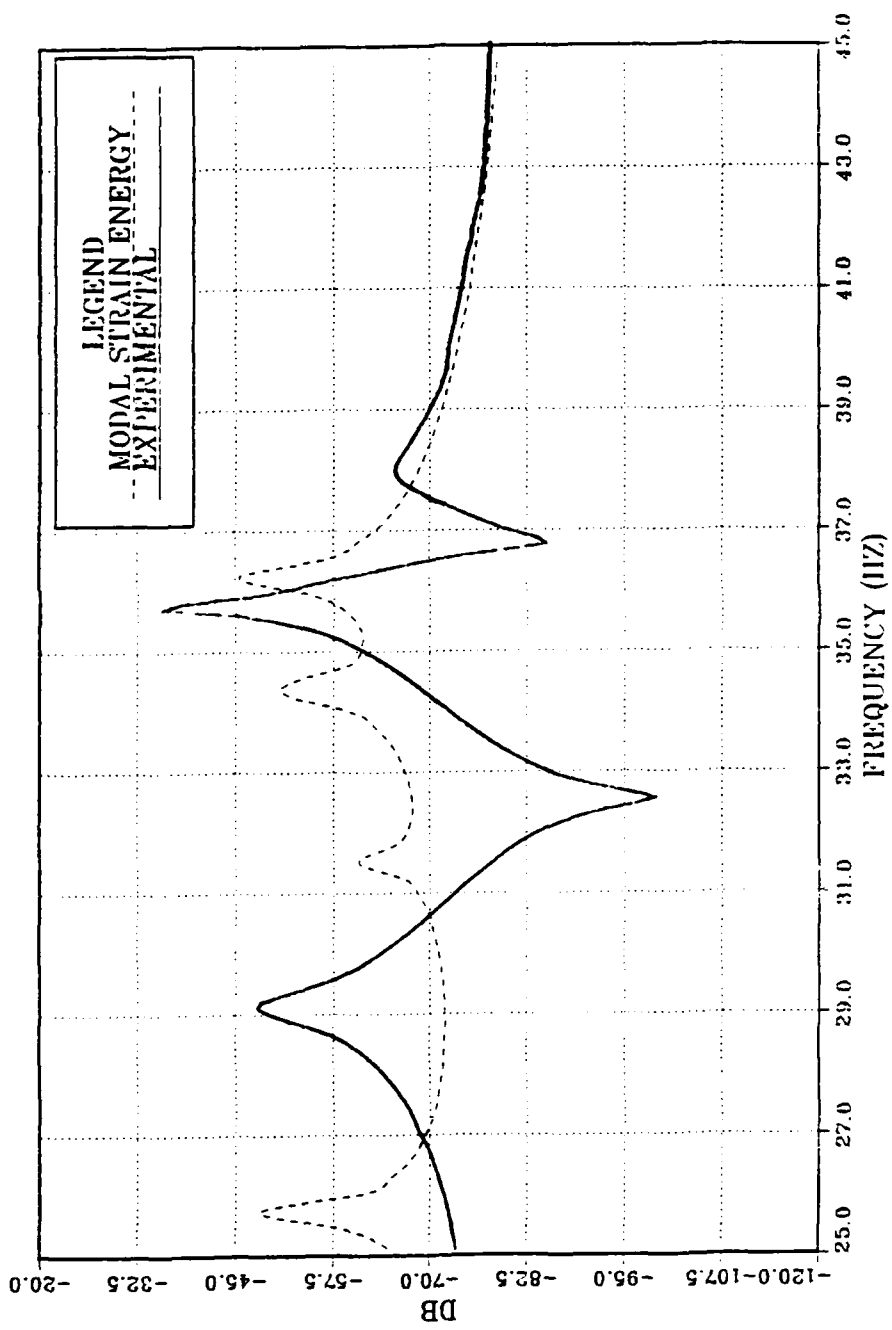


Figure 5.22. Modal Strain Energy method vs experimental frequency response, damping treatment applied to outer shell area, 25 to 45 Hz .

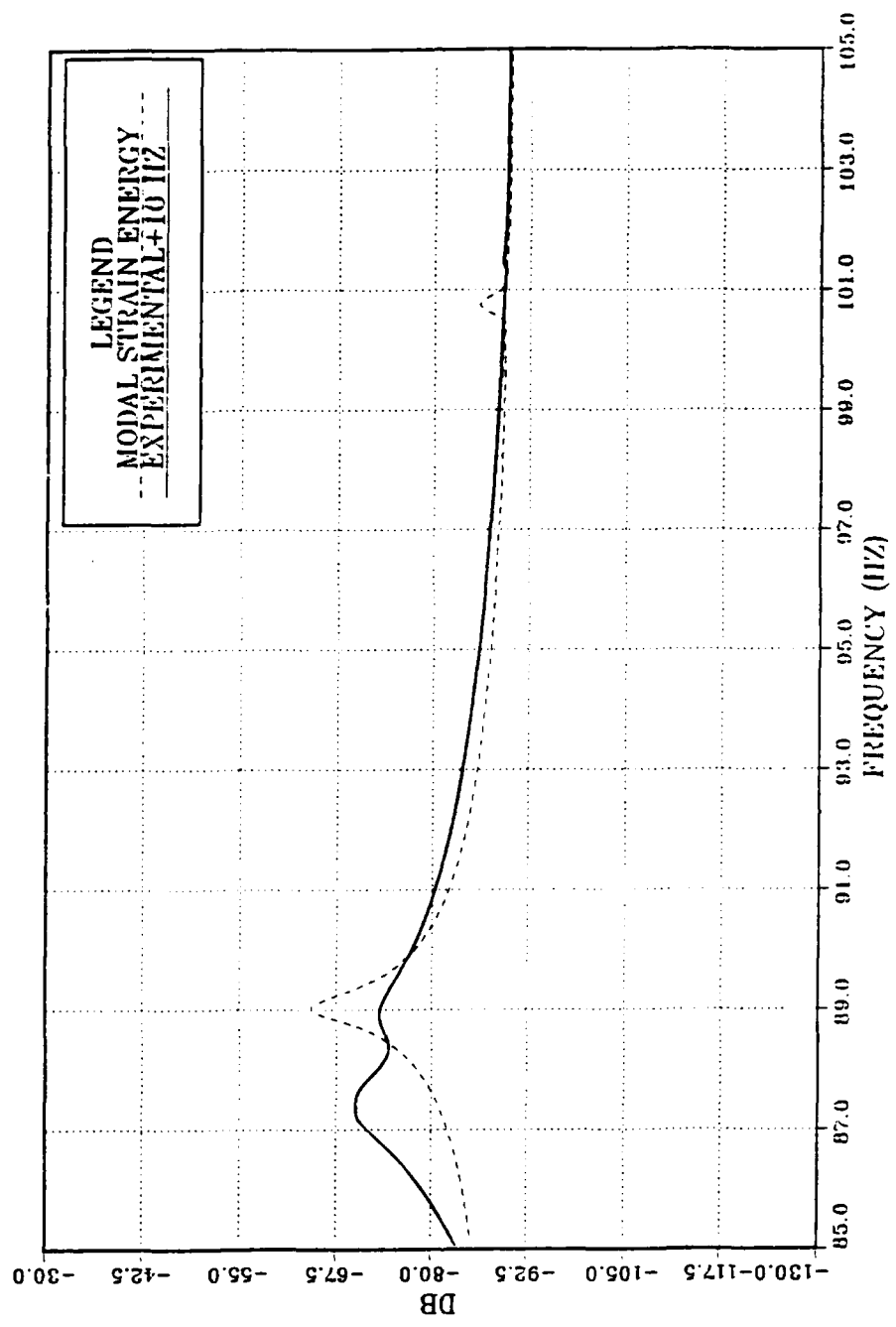
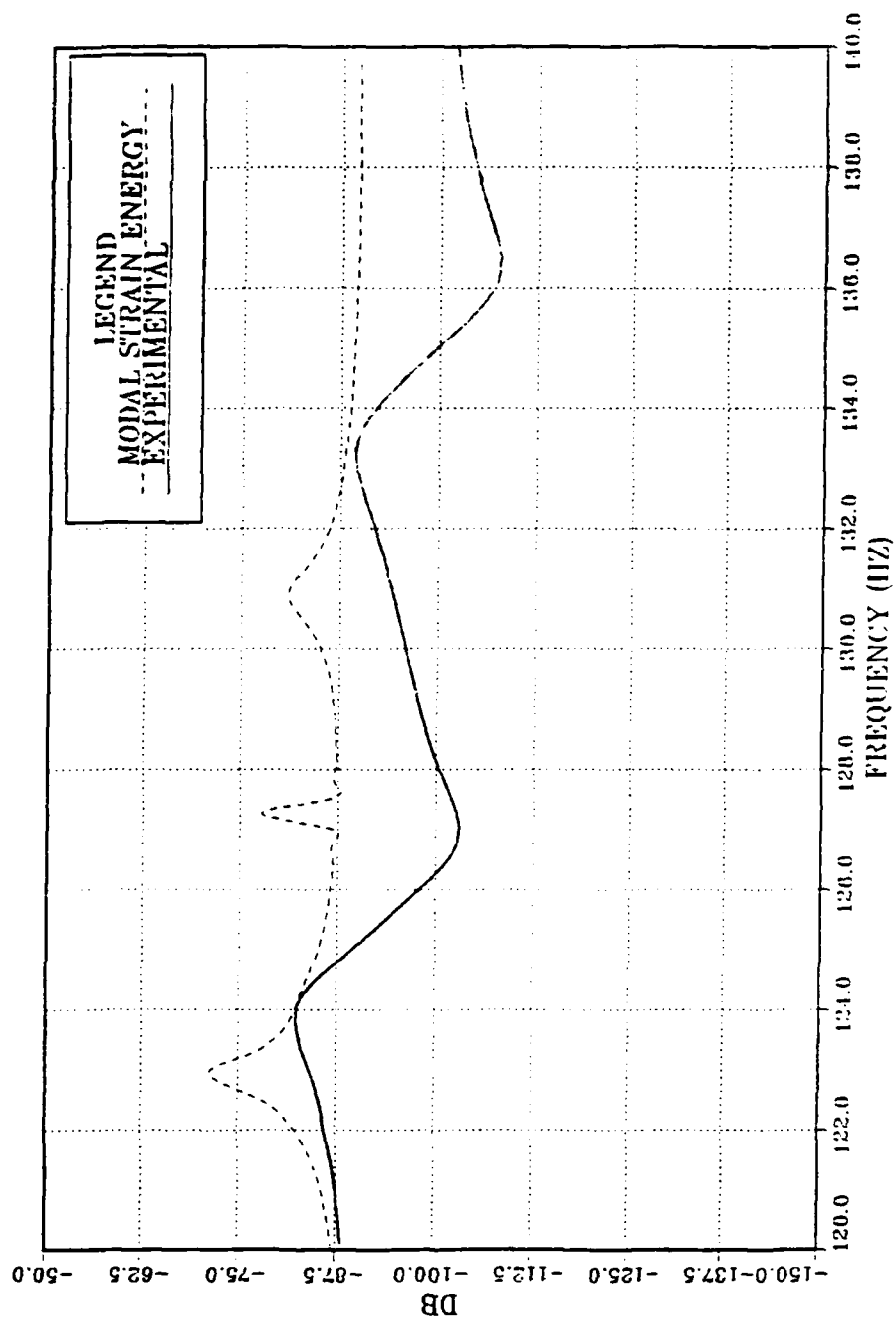


Figure 5.23. Modal Strain Energy method vs experimental frequency response, damping treatment applied to outer shell area, 95 to 115 Hz .



**Figure 5.24. Modal Strain Energy method vs experimental frequency response, damping treatment applied to outer shell area, 120 to 140 Hz .**

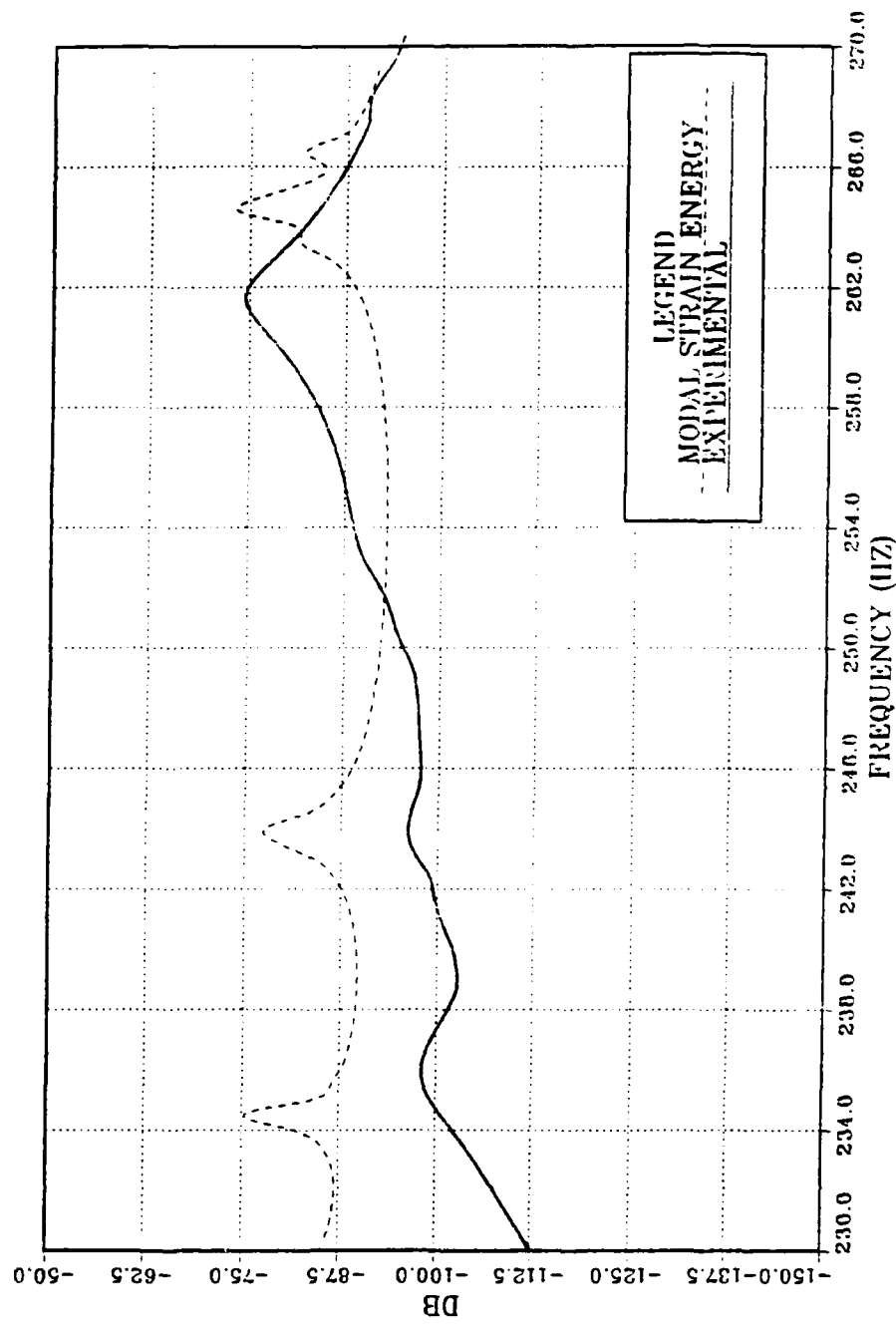


Figure 5.25. Modal Strain Energy method vs experimental frequency response, damping treatment applied to outer shell area, 230 to 270 Hz .

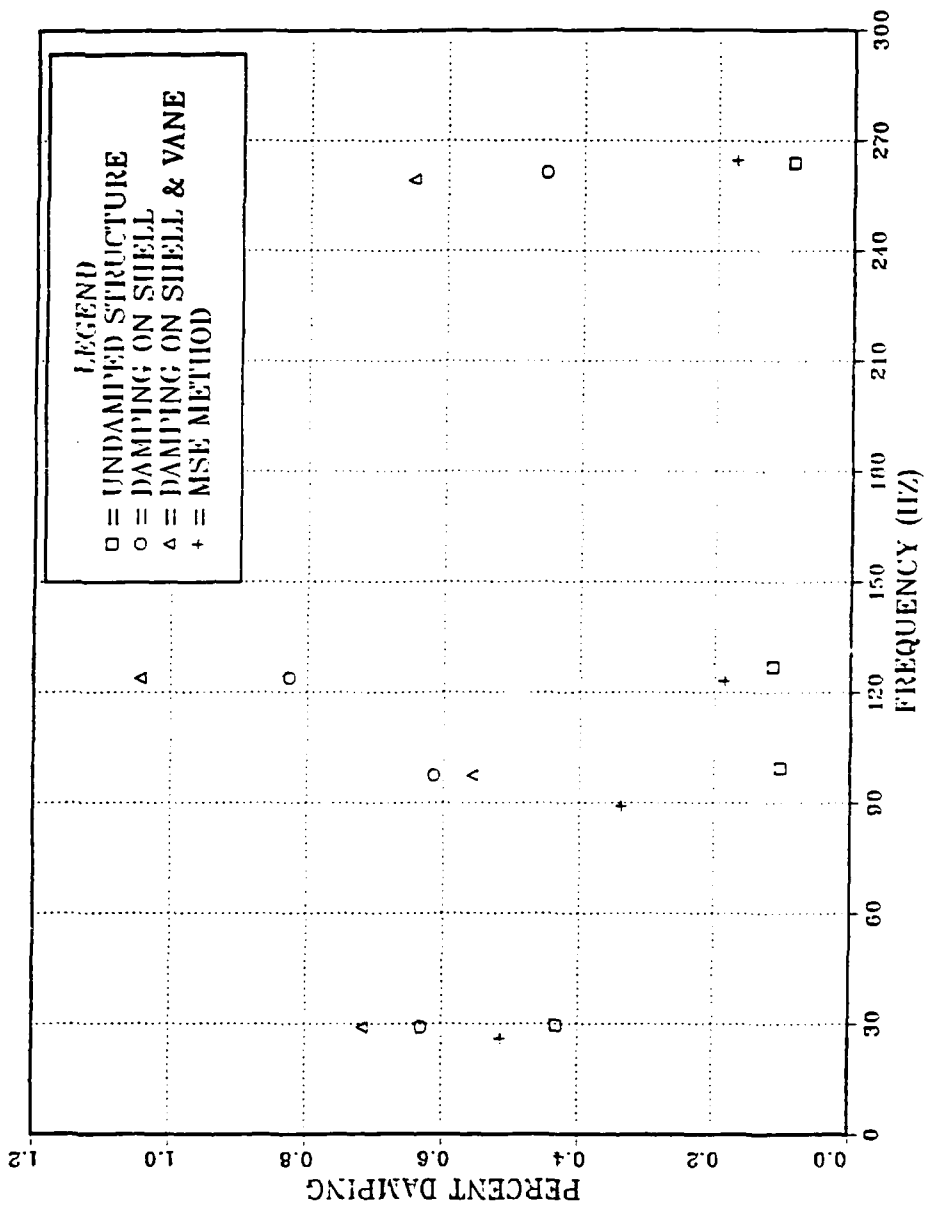


Figure 5.26. Structural damping in percent of critical damping.

## VI. CONCLUSIONS

The addition of a constrained viscoelastic layer damping treatment to a large, lightly damped structure was found to be very effective in reducing unwanted structural vibrations. The large reduction of response magnitude was encouraging, especially considering the light weight of the applied damping treatment. The relatively poor performance of the damping treatment in the lowest fifth of the frequency range studied indicated that viscoelastic materials with low shear moduli in certain frequency ranges are not effective in absorbing vibrational energy.

The use of visual mode shape observation and strain energy analysis to determine suitable locations for damping treatments was found to be effective. These analyses predicted that the most damping would be obtained by placing a damping treatment on the outer shell and experimentation proved that prediction to be true. In addition, when the use of these analyses indicates that an area of a structure is a poor candidate for a damping treatment, simply adding more damping material to that area may provide only marginally more damping, and may not be effective in light of the added mass, expense, and time required for application.

The Modal Strain Energy method is a viable means of predicting the frequency response of a structure with an applied damping treatment. However, the finite element model itself must be refined enough and must be accurate enough to allow the MSE method to perform adequately. Indeed, the need to accurately model complex structures makes the MSE method all the more attractive since the MSE method requires only three modal analysis runs, while direct frequency response techniques may require many more runs than that to adequately describe the behavior of the structure. In addition, since frequency response analysis takes much more time than modal analysis, direct frequency response techniques would not be cost effective for many complex structures.

## VII. RECOMMENDATIONS

The test structure used in this investigation was very much like many modern structures in that it was large, complex and lightly damped. Thus, it is recommended that this structure be used as a test unit for further damping research. For instance, it has been suggested that concentrated dampers, similar to but smaller than the ones used on large buildings, be installed between the inner and outer shells of the test structure to take advantage of the relative motion between these two parts of the structure.\* Many other innovative damping treatments are possible for use on this test structure, and the instrumentation is in place to quickly record their effects.

A more refined and accurate finite element model of the test structure should be developed that includes the effects of the bolts. This could include the use of direct matrix input to model the added stiffness and mass of the bolts. Also, the use of singly curved shell elements could be used to more accurately model the inner and outer shells. Finally, an alternate method of modelling the viscoelastic material such as using beam elements instead of solid elements should be attempted. The MSE method can then be retested using that refined model for comparison to the experimental data obtained.

The use of multi-layered constrained layer damping treatments should be investigated. Multi-layered damping treatments can increase the

---

\* Conversation with Dr. Dwayne Nelson, 3M Corp., Minneapolis-St.Paul, MN, 8 Aug 1988.

amount of damping that can be obtained, and they can increase the conformability of the treatment since the constraining layers can be made of a less stiff material [Ref. 13]. The increased conformability of the treatment may make application easier and may therefore result in fewer bond imperfections between the treatment and the base structure.

## **APPENDIX A**

### **INPUT DATA SETS FOR MSC/NASTRAN FOR UNDAMPED STRAIN ENERGY ANALYSIS AND FOR DAMPED MODAL STRAIN ENERGY(MSE) ANALYSIS**

The major difference between the two sets of NASTRAN input data is that the second set includes another set of grid points above the outer shell. In between this second set of grid points and the original grid points are the solid CHEXA elements used to model the viscoelastic material. Also, in the second case the CQUAD4 elements in the outer shell and constraining layer are offset from the grid points to make room for the viscoelastic material.

```

ID SHELL,MODAL
SQL 3
TIME 480
CEND
ESE=ALL
echo = both
diso = NONE
method = 100
output(plot)
plotter nastran
paper size 14.0 by 10.0
axes x,y,z
set 1 = all
view 0.,0.,0.
find scale, origin 1, set 1
plot nodal deformation 0, 6 thru 11, set 1, origin 1, shape
plot, shape
begin bulk
.coord2c,1,,0.,0.,0.,-1.,0.,0.,tcoord
tcoord,0.,1.,0.
grid,1,1,9.975,0.,0.
=,*(1),=,=,*(45.),=
=(5)
grid,9,1,14.108,0.,0.
=,*(1),=,=,*(90.),=
=(2)
grid,13,1,18.242,0.,0.
=,*(1),=,=,*(90.),=
=(2)
grid,17,1,22.375,0.,0.
=,*(1),=,=,*(22.5),=
=(14)
grid,33,1,9.975,0.,5.
=,*(1),=,=,*(45.),=
=(6)
grid,41,1,14.108,0.,5.
=,*(1),=,=,*(90.),=
=(2)
grid,45,1,18.242,0.,5.
=,*(1),=,=,*(90.),=
=(2)
grid,49,1,22.375,0.,6.
=,*(1),=,=,*(22.5),=
=(14)

```

Figure A.1. MSC/NASTRAN data set for undamped strain energy run (Page 1).

```

grid,65,1,9.975,0.,12.
=,*(1),=,=,*(45.),=
=(6)
grid,73,1,14.108,0.,12.
=,*(1),=,=,*(30.),=
=(2)
grid,77,1,18.242,0.,12.
=,*(1),=,=,*(30.),=
=(2)
grid,81,1,22.375,0.,12.
=,*(1),=,=,*(22.5),=
=(14)
grid,97,1,9.975,0.,18.
=,*(1),=,=,*(45.),=
=(6)
grid,105,1,14.108,0.,18.
=,*(1),=,=,*(30.),=
=(2)
grid,109,1,18.242,0.,18.
=,*(1),=,=,*(30.),=
=(2)
grid,113,1,22.375,0.,18.
=,*(1),=,=,*(22.5),=
=(14)
quad4,1,10,1,33,34,?
=,*(1),=,*(1),*(1),*(1),*(1)
=(5)
=,8,10,8,40,33,1
=,9,10,33,65,56,34
=,*(1),=,*(1),*(1),*(1),*(1)
=(5)
=,16,10,40,72,65,33
=,17,10,65,77,98,66
=,*(1),=,*(1),*(1),*(1),*(1)
=(5)
=,24,20,72,104,97,65
=,25,20,1,9,41,33
=,*(1),=,*(2),*(1),*(1),*(2)
=(2)
=,29,20,9,13,45,41
=,*(1),=,*(1),*(1),*(1),*(1)
=(2)
=,33,20,13,17,49,45
=,*(1),=,*(1),*(4),*(4),*(1)
=(2)

```

Figure A.2. MSC/NASTRAN data set for undamped strain energy run (Page 2).

```

=,37,20,33,41,73,65
=,*(1),=,*(2),*(1),*(1),*(2)
=(2)
=,41,20,41,45,77,73
=,*(1),=,*(1),*(1),*(1),*(1)
=(2)
=,45,20,45,49,81,77
=,*(1),=,*(1),*(4),*(4),*(1)
=(2)
=,49,20,65,73,105,07
=,*(1),=,*(2),*(1),*(1),*(2)
=(2)
=,53,20,73,77,109,105
=,*(1),=,*(1),*(1),*(1),*(1)
=(2)
=,57,20,77,81,113,109
=,*(1),=,*(1),*(4),*(4),*(1)
=(2)
=,61,30,17,40,50,19
=,*(1),=,*(1),*(1),*(1),*(1)
=(13)
=,70,30,32,64,49,17
=,77,30,49,81,82,50
=,*(1),=,*(1),*(1),*(1),*(1)
=(13)
=,92,30,64,36,81,49
=,93,30,81,113,114,42
=,*(1),=,*(1),*(1),*(1),*(1)
=(13)
=,108,30,96,128,113,81
PARAM,NTMASS,0.00259
param,autospc,ves
mat1,20,15.+6.,0.34,0.29514
mat1,30,30.+6.,0.3,0.28350
oshell1,10,20,0.5,20,,20
oshell1,20,20,0.25,20,,20
oshell1,30,30,0.25,30,,30
eigr,100,naiv,0.,400.,,50,,+eigr
+eigr,mas
suport,1,123456
enddata

```

Figure A.3. MSC/NASTRAN data set for undamped strain energy run (Page 3).

```

ID 4SESHFL1,MODAL
SQL 3
TIME 480
CEND
set 1=51,73
echo = both
diss = 1
ESE=ALL
method = 100
outout(plot)
plotter nastran
paper size 14.0 by 10.0
axes x,y,z
set 1 = all
view,0.,0.,0.
find scale, origin 1, set 1
plot modal deformation 0, 6 thru 11, set 1, origin 1, shape
plot, shape
begin bulk
cord2c,1,,0.,0.,0.,-1.,0.,0.,tcord
+cord,0.,1.,0.
grid,1,1,9.975,0.,0.
=,*(1),=,=,*(45.),=
=(6)
grid,9,1,14.15,0.,0.
=,*(1),=,=,*(90.),=
=(2)
grid,13,1,18.325,0.,0.
=,*(1),=,=,*(90.),=
=(2)
grid,17,1,22.5,0.,0.
=,*(1),=,=,*(22.5),=
=(14)
grid,33,1,9.975,0.,6.
=,*(1),=,=,*(45.),=
=(6)
grid,41,1,14.15,0.,6.
=,*(1),=,=,*(90.),=
=(2)
grid,45,1,18.325,0.,6.
=,*(1),=,=,*(90.),=
=(2)
grid,49,1,22.5,0.,6.
=,*(1),=,=,*(22.5),=
=(14)

```

Figure A.4. MSC/NASTRAN data set for damped  
Modal Strain Energy analysis (Page 1).

```

grid,65,1,9.975,0.,12.
=,*(1),=,=,*(45.),=
=(6)
grid,73,1,14.15,0.,12.
=,*(1),=,=,*(90.),=
=(2)
grid,77,1,18.325,0.,12.
=,*(1),=,=,*(90.),=
=(2)
grid,81,1,22.5,0.,12.
=,*(1),=,=,*(22.5),=
=(14)
grid,97,1,9.975,0.,18.
=,*(1),=,=,*(45.),=
=(6)
grid,105,1,14.15,0.,18.
=,*(1),=,=,*(90.),=
=(2)
grid,109,1,18.325,0.,18.
=,*(1),=,=,*(90.),=
=(2)
grid,113,1,22.5,0.,18.
=,*(1),=,=,*(22.5),=
=(14)
grid,129,1,22.53,0.,0.
=,*(1),=,=,*(22.5),=
=(14)
grid,145,1,22.53,0.,6.
=,*(1),=,=,*(22.5),=
=(14)
grid,161,1,22.53,0.,12.
=,*(1),=,=,*(22.5),=
=(14)
grid,177,1,22.53,0.,18.
=,*(1),=,=,*(22.5),=
=(14)
caud4,1,10,1,33,31,2
=,*(1),=,*(1),*(1),*(1),*(1)
=(5)
=,8,10,8,40,33,1
=,9,10,33,65,56,34
=,*(1),=,*(1),*(1),*(1),*(1)
=(5)

```

Figure A.5. MSC/NASTRAN data set for damped  
Modal Strain Energy analysis (Page 2).

```

=,16,10,40,72,65,53
=,17,10,65,97,98,06
=,*(1),=,*(1),*(1),*(1),*(1)
=(5)
=,24,20,72,104,97,65
=,25,20,1,0,41,33
=,*(1),=,*(2),*(1),*(1),*(2)
=(2)
=,29,20,0,13,45,41
=,*(1),=,*(1),*(1),*(1),*(1)
=(2)
=,33,20,13,17,49,45
=,*(1),=,*(1),*(4),*(4),*(1)
=(2)
=,37,20,33,41,73,65
=,*(1),=,*(2),*(1),*(1),*(2)
=(2)
=,41,20,41,45,77,73
=,*(1),=,*(1),*(1),*(1),*(1)
=(2)
=,45,20,45,49,81,77
=,*(1),=,*(1),*(4),*(4),*(1)
=(2)
=,49,20,65,73,105,07
=,*(1),=,*(2),*(1),*(1),*(2)
=(2)
=,53,20,73,77,109,105
=,*(1),=,*(1),*(1),*(1),*(1)
=(2)
=,57,20,77,81,113,110
=,*(1),=,*(1),*(4),*(4),*(1)
=(2)
=,61,30,17,49,50,19,,,-0.125
=,*(1),=,*(1),*(1),*(1),*,,-0.125
=(13)
=,76,30,32,54,49,17,,,-0.125
=,77,30,49,41,82,50,,,-0.125
=,*(1),=,*(1),*(1),*(1),*(1),*,,-0.125
=(13)
=,92,30,64,96,81,49,,,-0.125
=,03,30,81,113,114,82,,,-0.125
=,*(1),=,*(1),*(1),*(1),*(1),*,,-0.125
=(13)

```

Figure A.6. MSC/NASTRAN data set for damped  
Modal Strain Energy analysis (Page 3).

```

=,108,30,96,128,113,81,,0.125
=,109,50,129,145,145,130,,0.02
=,*(1),=,*(1),*(1),*(1),,0.02
=(13)
=,124,50,144,160,145,129,,0.02
=,125,50,145,161,162,146,,0.02
=,*(1),=,*(1),*(1),*(1),,0.02
=(13)
=,140,50,160,176,161,145,,0.02
=,141,50,161,177,178,162,,0.02
=,*(1),=,*(1),*(1),*(1),,0.02
=(13)
=,156,50,176,192,177,161,,0.02
cnexa,157,60,17,49,50,18,129,145,+01
=,*(1),=,*(1),*(1),*(1),*(1),*(1),*(1)
=(13)
+01,146,130
*(1),*(1),*(1)
=(13)
chexa,172,60,32,64,49,17,144,160,+016
+016,145,129
chexa,173,60,49,81,82,50,145,161,+017
=,*(1),=,*(1),*(1),*(1),*(1),*(1),*(1)
=(13)
+017,162,145
*(1),*(1),*(1)
=(13)
chexa,198,60,54,90,81,49,160,176,+032
+032,161,145
chexa,189,60,81,113,114,82,161,177,+033
=,*(1),=,*(1),*(1),*(1),*(1),*(1),*(1)
=(13)
+033,178,162
*(1),*(1),*(1)
=(13)
cnexa,204,60,96,128,113,81,175,192,+048
+048,177,161
PARAM,41MASS,0.00259
param,autosec,yes
mat1,20,15.+6,,0.34,0.29514
mat1,30,30.+6,,0.3,0.28350
mat1,40,10.+6,,0.33,0.0984
mat1,50,,150.0,0.49,0.035,,1.0

```

Figure A.7. MSC/NASTRAN data set for damped  
Modal Strain Energy analysis (Page 4).

```
osnel,19,20,0.5,20,,20
oshell,20,20,0.25,20,,20
oshell,30,30,0.25,30,,30
oshell,50,40,0.04,40,,40
psolid,60,50,1
eiar,100,nniv,0.,500.,.,.,+eiar
+eiar,mass
support,1,123456
enddata
```

Figure A.8. MSC/NASTRAN data set for damped  
Modal Strain Energy analysis (Page 5).

## APPENDIX B

### **FORTRAN PROGRAM USED TO COMPUTE LOSS FACTORS FOR THREE LAYER SYSTEM**

Calculations of loss factors for the three layer subsystem used to determine damping material thicknesses were performed using a FORTRAN program. The program used to perform these calculations is shown in this appendix. The program reads in values from a data table of shear modulus and loss factor versus temperature for 3M ISD-112, and outputs the loss factor of the composite system. Each run of the program supplied data of loss factor versus temperature for eight values of constraining layer thickness. These values would then be plotted as shown in Figures 3.9 through 3.11, for different values of viscoelastic material thickness.

```

PROGRAM CARPET
*****  

* PROGRAM CARPET PRODUCED BY LT. JAMES R. NAULT USN . THIS PROGRAM *  

* READS IN THE VALUES OF LOSS FACTOR AND SHEAR MODULUS FOR ISD-112 *  

* AND USES THESE VALUES TO COMPUTE A CARPET PLOT FOR THE SYSTEM OF *  

* INTEREST.  

*****  

REAL F,FR0M,MROM,N,ML,ETAFR0,SL,SH,FROL,C,T0,TEMP,A,LOGFR,FR  

REAL LOGM,M,LOGETA,ETA2,LOGET1,H1,E1,H2,H3,E3,K,G,LITA,LITB  

REAL ETAS(8),EHCCUBE,E,H,H31,AREL,AIMG,PI  

* ASSIGN FREQUENCY OF INTEREST VALUE  

F=29.70  

* COMPUTE PI  

PI=4.0*ATAN(1.0)  

* ASSIGN CONSTANT VALUES FOR STRUCTURE  

H1=0.25  

E1=30000000.0  

E3=10000000.0  

K=PI/35.3  

H2=0.030  

* READ IN MODULUS AND LOSS FACTOR FOR ISD-112  

DO 10 J=0,100  

READ*,TEMP,M,ETA2  

* COMPUTE SYSTEM YOUNG'S MODULUS AND SYSTEM LOSS FACTOR  

DO 20 I=1,8  

H3=REAL(I)/200.0  

H=H1+H2+H3  

H21=(H1+H2)/2.0  

H31=(H1+2.0*H2+H3)/2.0  

G=M/(E3*XH3*XH2*K**2)  

E2=3.0*M  

LITA=E1*XH1+G*(E1*XH1+E3*XH3)  

LITB=ETA2*XG*(E1*XH1+E3*XH3)  

AREL=G*X1*XH1*X3*XH3*XH31**2*(LITA+ETA2*XLTB)  

AIMG=G*X1*XH1*X3*XH3*XH31**2*(ETA2*XLTB)  

BREL=E1*XH1*X2*XH2*XH31*(LITA+LTB*ETA2)  

BIMG=E1*XH1*X2*XH2*XH31*(LITA*ETA2-LTB)  

CREL=2*XG*X2*XH2*X3*XH3*XH21*XH31*(LITA*(1-ETA2**2)+2*XLTB  

*ETA2)  

CIMG=2*XG*X2*XH2*X3*XH21*XH31*(2*XLTB*ETA2-LTB*X  

ETA2**2)  

EHCCUBE=E1*XH1**3+E3*XH3**3+12.0*(AREL-BREL-CREL)/(LITA  

**2+LTB**2)  

E=EHCCUBE/(H**3)  

ETAS(I)=12.0*(AIMG-BIMG-CIMG)/((LITA**2+LTB**2)  

*EHCCUBE)
20    CONTINUE
      PRINT 15,TEMP,ETAS(1),ETAS(2),ETAS(3),ETAS(4)
      ,ETAS(5),ETAS(6),ETAS(7),ETAS(8)
15    FORMAT(1X,F6.1,2X,8F09.5)
10    CONTINUE
END

```

Figure B.1. FORTRAN program to calculate system loss factor.

## **LIST OF REFERENCES**

1. Johnson, C.D. and Kienholz, D.A., "Finite Element Prediction of Damping in Structures with Constrained Viscoelastic Layers," AIAA Journal, Vol.20, No.9, September 1982.
2. Maurer, G.J., Vibration Response of Constrained Viscoelastically Damped Plates: Analyses and Experiments M.S. Thesis, Naval Postgraduate School, Monterey, California, December 1987.
3. Thompson, W.T., Theory of Vibration with Applications, Prentice-Hall, 1981.
4. Nashif, A.D., Jones, D.I.G. and Henderson, J.P., Vibration Damping, Wiley-Interscience Publications, John Wiley and Sons, 1985.
5. Johnson, C.D. and Kienholz, D.A., "Design and Testing of a Sixty-Foot Damped Generic Space Truss," Damping 1986 Proceedings, Flight Dynamics Laboratory, Air Force Wright Aeronautical Laboratories, Air Force System Command, Wright-Patterson Air Force Base, Ohio.
6. Iverson, J.C., Experimental Investigation of Damping Characteristics of Bolted Structural Connections for Plates and Shells M.S. and Mechanical Engineer Thesis, Naval Postgraduate School, Monterey, California, September 1987.
7. Durham, R.C., Experimental Investigation of the Effects of Underwater Exposure on the Damping Characteristics of Bolted Structural Connections for Plates and Shells M.S. Thesis, Naval Postgraduate School, Monterey, California, March 1988.
8. Reismann, H. and Pawlik, P.S., Elasticity Theory and Applications, Wiley-Interscience Publications, John Wiley and Sons, 1980.
9. Department of the Navy, Principles and Applications of Underwater Sound, Headquarters, Naval Material Command, Washington, DC , 1968.

10. Kluesener, M.F., "Design of a Damped Electronic Support Panel," Vibration Damping Short Course Notes, Section 10, University of Dayton, Ohio, June 1987.
11. Graf, P.A., Drake, M.L., Bouchard, M.P. and Dominic, R.J., "Passive Damping - Sonic Fatigue - and the KC - 135," Vibration Damping Short Course Notes, Appendix B, University of Dayton, Ohio, June 1987.
12. University of Dayton Research Institute, "Fundamentals of Damping Treatment," Vibration Damping Short Course Notes, Section 6, University of Dayton, Ohio, June 1987.
13. Drake, M.L., "Design Techniques Fourth Order Beam Theory," Vibration Damping Short Course Notes, Section 7, University of Dayton, Ohio, June 1987.
14. Reinhall, P.G. and Miles, R.N., "Effects of Bond Imperfections on the Dynamic Response of Laminated Beams," Damping 1986 Proceedings, Flight Dynamics Laboratory, Air Force Wright Aeronautical Laboratories, Air Force System Command, Wright-Patterson Air Force Base, Ohio.
15. Schaeffer, H.G., MSC/NASTRAN Primer Static and Normal Modes Analysis, Wallace Press, Inc., 1982.
16. Drake, M.L. and Kluesener, M.F., "Damping Predictions using Material Properties from Various Test Methods," Vibration Damping Short Course Notes, Section GB, University of Dayton, Ohio, June 1987.

## INITIAL DISTRIBUTION LIST

- |    |   |   |
|----|---|---|
| 1. | Defense Technical Information Center<br>Cameron Station<br>Alexandria, Virginia 22304-6145  | 2 |
| 2. | Library, Code 0142<br>Naval Postgraduate School<br>Monterey, California 93943-5004  | 2 |
| 3. | Dean of Science and Engineering, Code 06<br>Naval Postgraduate School<br>Monterey, California 93943-5004                                | 2 |
| 4. | Research Administrations Office, Code 012<br>Naval Postgraduate School<br>Monterey, California 93943-5004                               | 1 |
| 5. | Department Chairman, Code 69<br>Department of Mechanical Engineering<br>Naval Postgraduate School<br>Monterey, California 93943-5004    | 1 |
| 6. | Professor Y. S. Shin, Code 69Sg<br>Department of Mechanical Engineering<br>Naval Postgraduate School<br>Monterey, California 93943-5004 | 3 |
| 7. | Dr. K.S. Kim, Code 69Ki<br>Department of Mechanical Engineering<br>Naval Postgraduate School<br>Monterey, California 93943-5004         | 1 |
| 8. | Dr. Arthur Kilcullen, Code 1962<br>David W. Taylor Naval Ship R&D Center<br>Bethesda, Maryland 20084                                    | 5 |
| 9. | Dr. Lawrence Maga, Code 196<br>David W. Taylor Naval Ship R&D Center<br>Ship Acoustics Department (196)<br>Bethesda, Maryland 20084     | 1 |

- |     |  |   |
|-----|--|---|
| 10. | Mr. Maurice Sevik, Code 19<br>David W. Taylor Naval Ship R&D Center<br>Bethesda, Maryland 21402  | 1 |
| 11. | Mr. Gordon Eversteine, Code 1844<br>David W. Taylor Naval Ship R&D Center<br>Bethesda, Maryland 20084  | 1 |
| 12. | Dr. B. Whang, Code 1750.2<br>David W. Taylor Naval Ship R&D Center<br>Hull Group Head, Submarine Protection Division<br>Bethesda, Maryland 20084     | 1 |
| 13. | Dr. Peter Doubleday<br>Underwater Sound Research Detachment<br>Naval Research Laboratory<br>P.O. Box 8337<br>Orlando, Florida 32856                  | 1 |
| 14. | Mr. Bob Ting<br>Underwater Sound Research Detachment<br>Naval Research Laboratory<br>P.O. Box 8337<br>Orlando, Florida 32856                         | 1 |
| 15. | Dr. Alfred Tucker<br>Office of Naval Research<br>800 North Quincy St.<br>Arlington, Virginia 22217   | 1 |
| 16. | Mr. P. Majumdar, Code 55N<br>Naval Sea Systems Command Headquarters<br>Washington, D.C. 20362  | 1 |
| 17. | Mr. Jerry Snyder, Code 55Y13<br>Naval Sea Systems Command Headquarters<br>Washington, D.C. 20362   | 1 |
| 18. | Mr. Walter Madigosky<br>White Oak Laboratory<br>Naval Surface Weapons Center Detachment<br>10901 New Hampshire Ave.<br>Silver Spring, Maryland 20903 | 1 |

- |   |   |
|---|---|
| 19. Dr. N. T. Tsai<br>Defense Nuclear Agency<br>SPSS<br>Washington, D.C. 20305-1000   | 1 |
| 16. Dr. P. Mahmoodi<br>3M Company<br>Corporate Research Laboratories / 3M<br>Building 201 - BS - 08<br>St. Paul, Minnesota 55144    | 1 |
| 17. Dr. D. Nelson<br>3M Company<br>Corporate Research Laboratories / 3M<br>Building 230 - 1F - 02<br>St. Paul, Minnesota 55144-1000 | 1 |